SUPPORTING INFORMATION FOR

Cationic Guest Inclusion in Widemouthed Schiff Base Macrocycles

*Jian Jiang and Mark J. MacLachlan**

Department of Chemistry, University of British Columbia, 2036 Main Mall, Vancouver BC V6T 1Z1, Canada

mmaclach@chem.ubc.ca

Table of Contents

Figures

Experimental

Materials

Cyclobis(paraquat-*p*-phenylene) hexafluorophosphate **CBPQT**$^{4+}$·4PF_6 [1] and macrocycles **1** and **2** were synthesized by literature methods.[2] Cetylpyridinium chloride **3**$^{+}$·Cl^{-}, cetyltrimethylammonium bromide **4**$^{+}$·Br^{-}, tetrabutylammonium bromide **5**$^{+}$·Br^{-}, methyl viologen dichloride **6**$^{2+}$·2Cl^{-}, tetraphenylphosphonium bromide, pyridine, diethylamine, and 4,4'-bipyridine were obtained from standard suppliers and used without further purification. Deuterated solvents were purchased from Cambridge Isotope Laboratories.

Equipment

^{1}H and ^{13}C NMR spectra were recorded on a Bruker AV-400 spectrometer. ^{13}C NMR spectra were recorded using a proton decoupled pulse sequence. UV-vis spectra were obtained on a Varian Cary 5000 UV-vis/near-IR spectrophotometer using a 1 cm quartz cuvette. IR spectra were obtained as KBr discs with a Bomems MB-series spectrometer. MALDI-TOF mass spectra were obtained in a dithranol matrix (cast from THF) on a Brüker Biflex IV instrument where spectra were acquired in the positive reflection mode with delay extraction. Melting points were obtained on a Fisher-John's melting point apparatus.

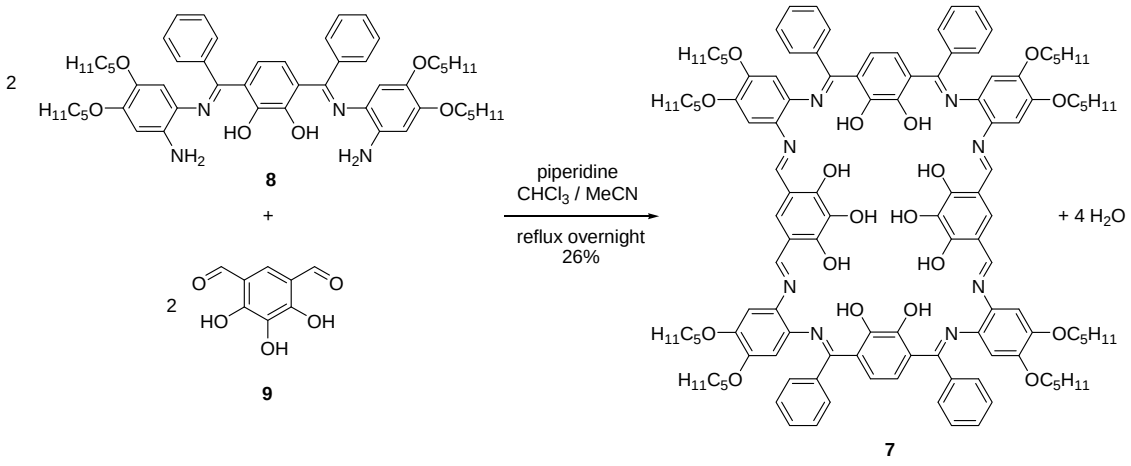

Scheme S1. Synthesis of Macrocycle **7**.

Synthesis of Macrocycle 7

Compound **8**[2] (0.150 g, 0.18 mmol) and compound **9**[3] (0.032 g, 0.18 mmol) were dissolved in 100 mL of dry, degassed chloroform and 50 mL of dry, degassed acetonitrile. After the red solution was stirred at room temperature for 5 min,

piperidine (0.04 mL, 0.41 mmol) was added, resulting in a darkening of the solution. The resulting mixture was heated at reflux under nitrogen overnight. After cooling to room temperature, the solution was concentrated to a few mLs by rotary evaporation. Addition of methanol yielded a red precipitate that was isolated by filtration. Recrystallization from chloroform/methanol afforded pure **7** (0.046 g, 0.023 mmol) as a red solid in 26% yield. ^{1}H NMR ($CDCl_3$) : δ 14.53 (s, 4H), 14.39 (s, 4H), 8.31 (s, 4H), 7.11- 7.25 (m, 22H), 6.90 (s, 2H), 6.73 (s, 4H), 6.42 (s, 4H), 6.33 (s, 4H), 3.95 (t, 8H), (t, 8H), 0.90-1.98 (m, 88H) ppm; ^{13}C NMR ($CDCl_3$) : δ 176.0, 157.9, 154.5, 153.7, 149.5, 148.0, 137.3, 135.9, 134.6, 131.6, 129.8, 129.7, 128.8, 122.0, 121.0, 114.1, 109.7, 103.4, 78.2, 70.9, 70.3, 30.0, 29.7, 29.2, 29.1, 23.5, 23.4, 15.0 ppm; IR: υ = 3500, 3055, 2952, 2929, 2859, 1605, 1583, 1494, 1443, 1417, 1379, 1329, 1256, 1209, 1151, 1073, 1039, 984, 920, 889, 854, 803, 774, 701, 573, 463 cm^{-1}; UV-vis (CH_2Cl_2) : λ_{max} (ε) = 376 (4.96×10^4), 315 (5.75×10^4) nm (L mol^{-1} cm^{-1}); MALDI-TOF-MS: m/z 1979.1 $[M+H]^+$; HRMS (ESI): $C_{120}H_{137}N_8H_{18}$ Calc'd: 1978.0051, Found: 1978.0068; m.p.= 245 °C (dec.).

NMR experiments

Job plots (Continuous variation method)

The stoichiometry of each host-guest complex was determined by Job's methods of continuous variations.[4] Host and guest compounds were dissolved in deuterated solvent in NMR tubes, in which the total concentration of host and guest was kept constant. Normally, the molar fraction of host and guest in the resulting solution in NMR tubes varied from 0.1 to 0.9. The changes in chemical shifts (Δδ) were multiplied by molar fraction and plotted against molar fraction to obtain the Job plot.

NMR titrations

The host macrocycle was dissolved in an appropriate amount of deuterated solvent in a vial. 400 μL of the resulting solution was added into an NMR tube. The guest compound was dissolved in the host solution in the vial to form a host-guest solution. By microsyringe, the host-guest solution was added, in calculated amount, into the NMR tube which originally contains 400 μL host solution. The ^{1}H NMR experiments were continued until no significant change in chemical shift was observed in successive ^{1}H NMR spectra. Binding constant was calculated by nonlinear curve fitting methods for the guest-induced chemical shifts of the selected peaks.[5]

Simulations

Given the large size of the macrocycles in this study, their flexibility, and the number of interactions involved (hydrogen-bonding, π-π stacking, electrostatic), detailed DFT calculations were beyond the scope of the study. However, we employed semi-empirical calculations (pm3) to estimate the size of the macrocycles, to determine the expected conformations, and to model the host-guest interactions to correlate with experiments. Calculations were performed on macrocycles **1** and **2** using Spartan '04 for Windows (note that peripheral alkoxy groups were removed for simplification as they are not expected to significantly affect the conformation). For each macrocycle, simulations were started from several different likely conformations and minimized. Figures S1-S3 show a series of energy-minimized structures obtained from semi-empirical calculations of macrocycles **1** and **2**, respectively, along with the energies. There may well be additional conformation representing minima on a complex conformational landscape, but these are representative.

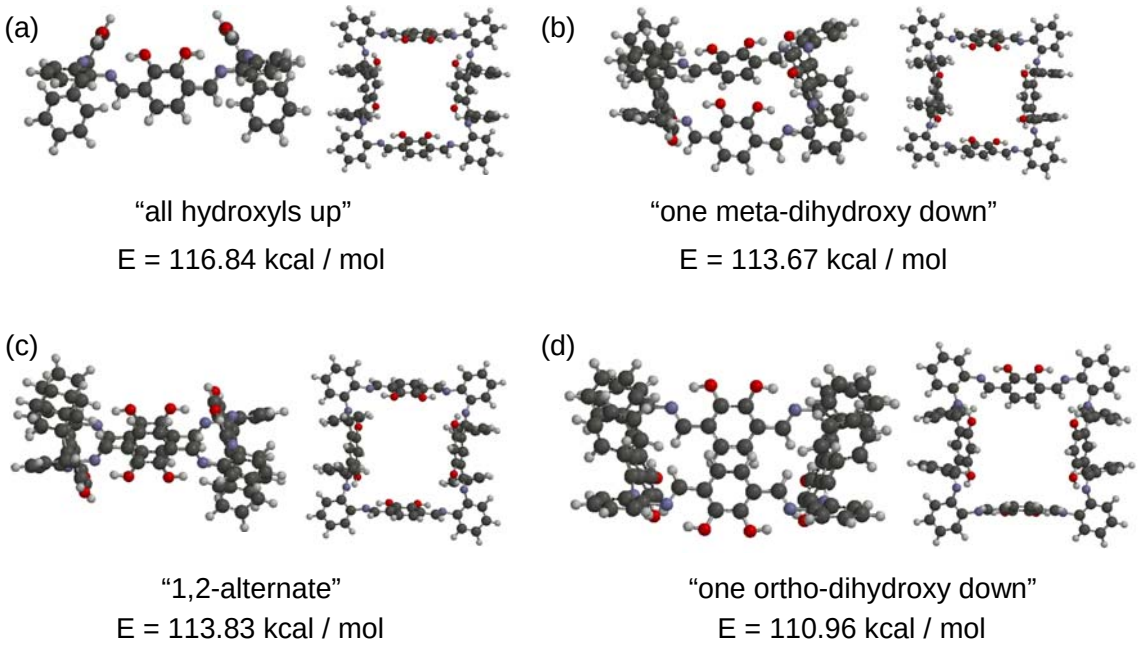

Figure S1. Representative energy-minimized conformations of macrocycle **1** as deduced by semi-empirical (PM3) measurements. The energy of the conformation is shown beneath each structure. The structure shown in the paper is the "1,3-alternate" with E = 111.14 kcal / mol. (Nomenclature from calixarene chemistry.)

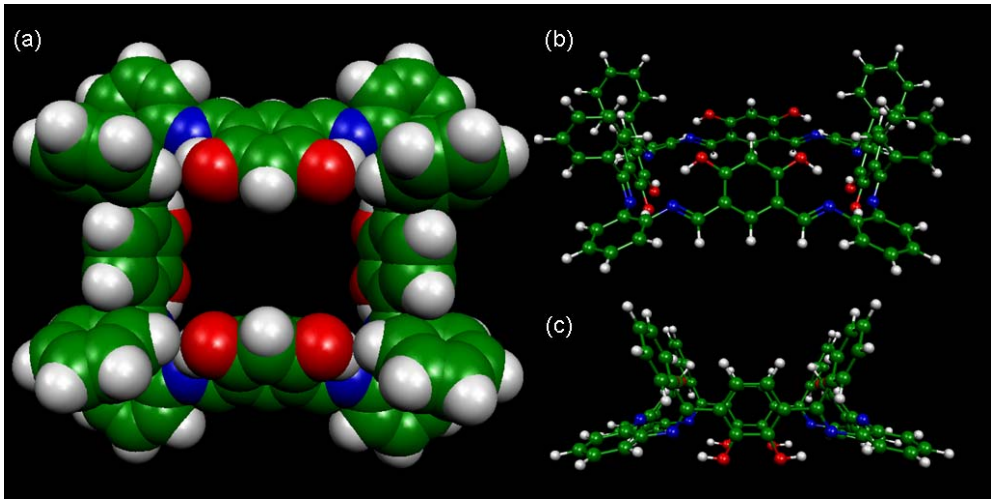

Figure S2. Energy minimized (pm3) structure of **2** (a) space-filling view; (b,c) side views. The energy of this conformation (the "1,3-alternate") is E = 110.10 kcal / mol. (The alkoxy chains of the macrocycle are not shown as they were not included in the calculation.)

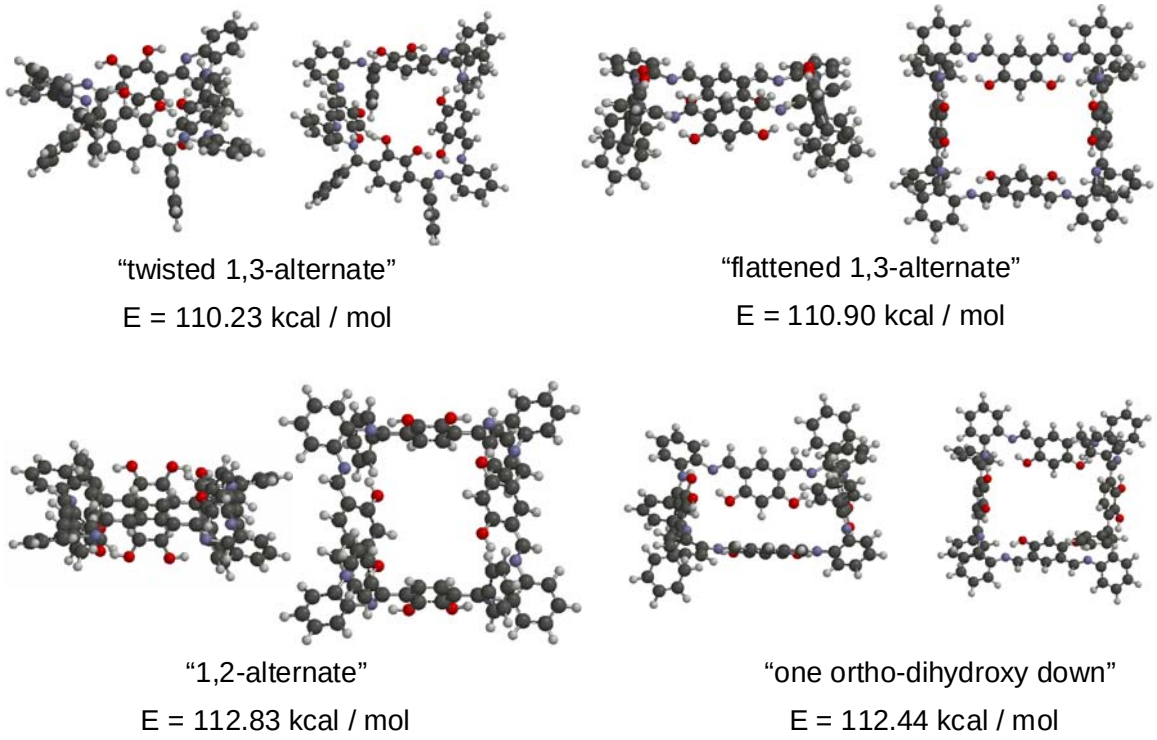

Figure S3. Representative energy-minimized conformations of macrocycle **2** as deduced by semi-empirical (PM3) measurements.

Energy-minimized structures of the host-guest complexes were examined in a similar way. The guest was incorporated into the interior of the macrocycle starting with different orientations of the guest and different conformations of the host. There are many stable structures. The conformation illustrated in Figure S4 is a representative, energy-minimized structure, and does not represent a global minimum.

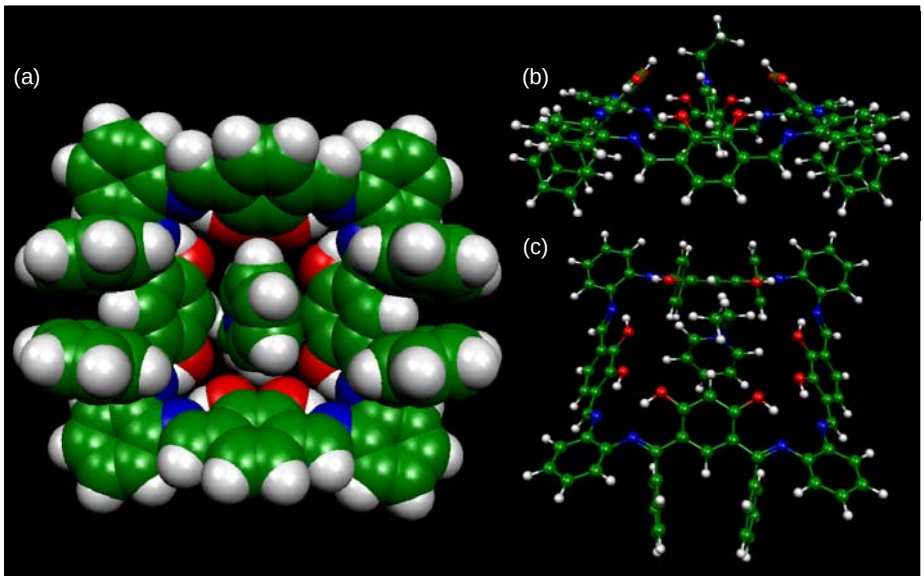

Figure S4. Energy-minimized (PM3) model of $\mathbf{3}^{+}\subset\mathbf{1}$ complex (a) space-filling view from bottom; (b,c) side views. (The alkoxy chains of **1** were removed for calculation and the alkyl chain of $\mathbf{3}^{+}$ was truncated to ethyl.)

The $\mathbf{CBPQT}^{4+}\subset\mathbf{7}$ complex was modeled to see that the guest would fit inside macrocycle **7**, and to orient it in a way that explains the correlations seen in the 2-D ROESY ^{1}H NMR spectrum (Figure S28). Figure S5 below shows the model.

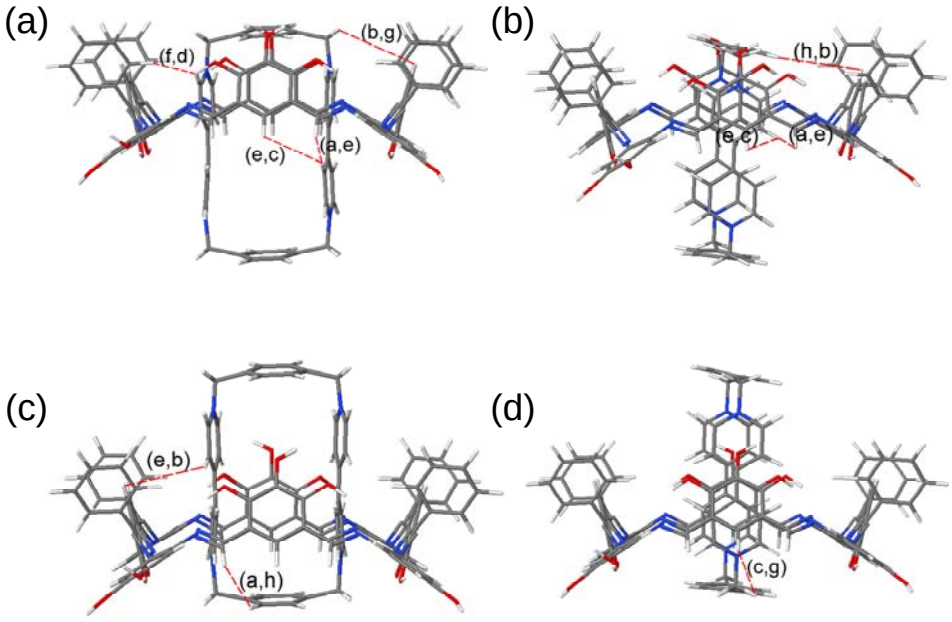

Figure S5. The assignment of spin-couplings and the corresponding conformations for the $\mathbf{CBPQT}^{4+}\subset\mathbf{7}$ complex. (The guest in structure (a) rotates 90º to give (b) and the guest in (c) rotates 90º to give (d). The alkoxy chains are omitted for clarity.) The structures shown are models that account for the observed ROESY spectrum, not calculated conformations.

NMR Peak Assignments for Macrocycle 1

In order to understand the 2-D ROESY NMR spectra for guest binding inside macrocycles **1** and **2**, it was first necessary to assign most of the protons in the NMR spectrum for macrocycle **1**. Shown below is the 1-D NMR spectrum (Figs S6 and S7).

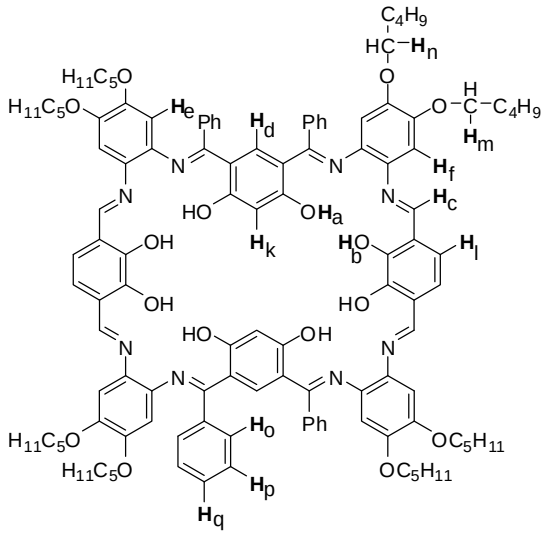

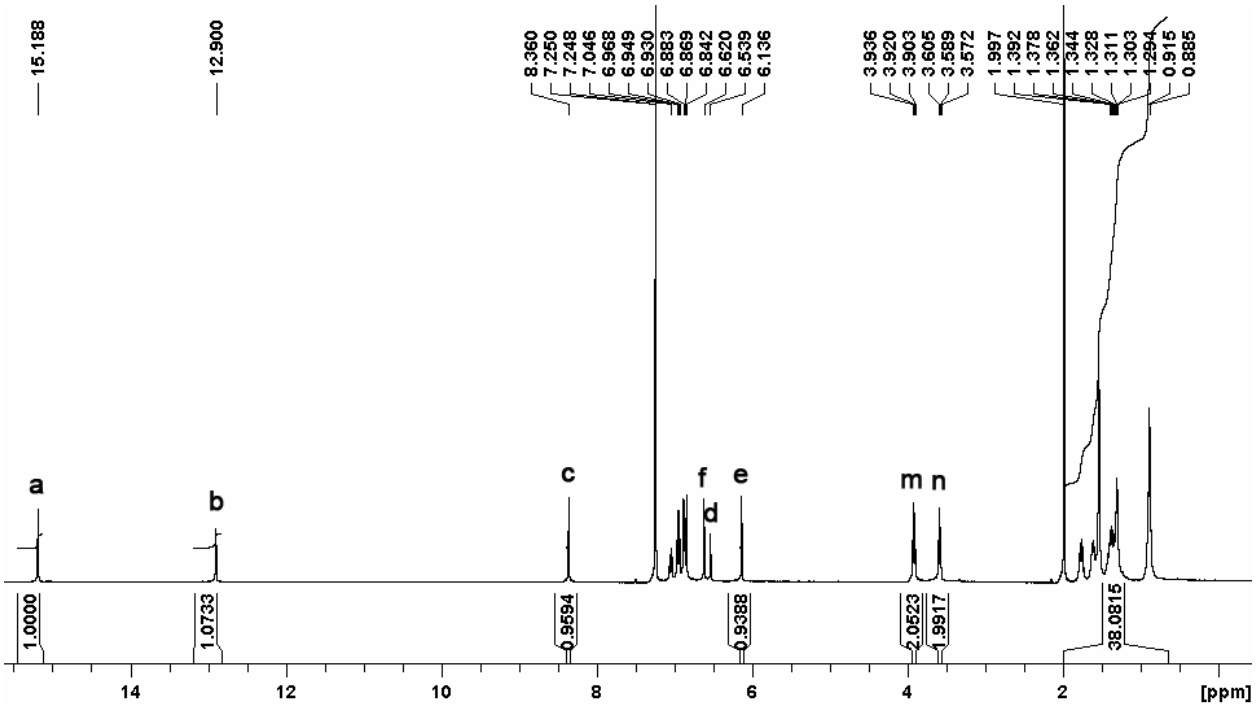

Figure S6. ^{1}H NMR Spectrum of macrocycle **1**.

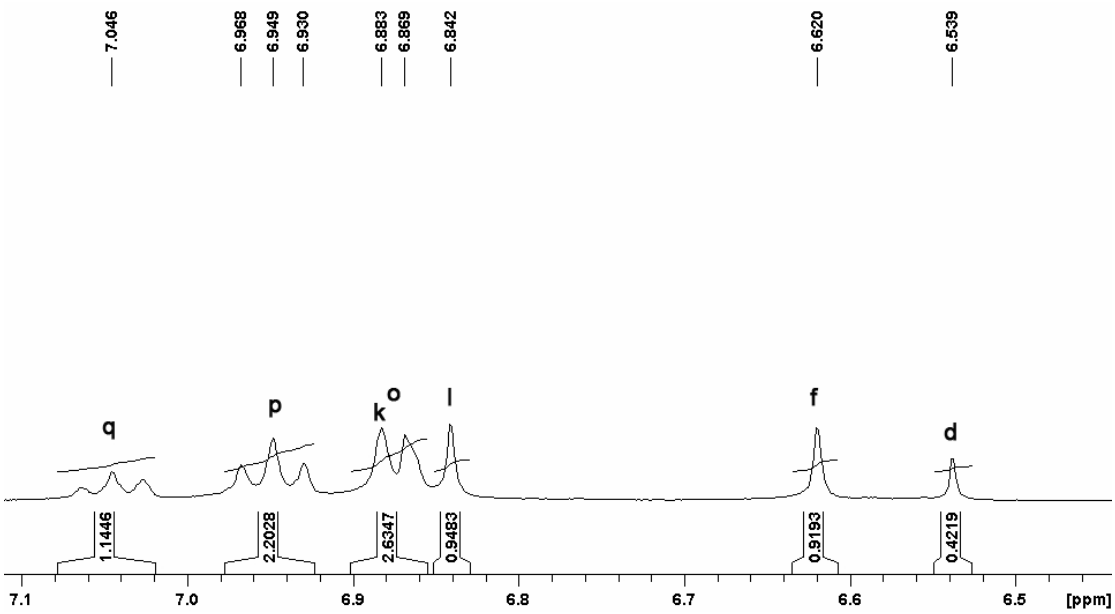

Figure S7. ^{1}H NMR Spectrum of the macrocycle **1** between 6.5-7.1 ppm.

Macrocycle **1** was synthesized from a resorcinol-containing precursor and 3,6-diformylcatechol. The chemical shift of hydroxyl protons of resorcinol-containing precursor is 15.74 ppm[2], while macrocycles made from 3,6-diformylcatechol always[6] have OH proton resonances near 13 ppm[7] in $CDCl_3$. Based on these, we assigned the peak at 15.19 ppm and 12.90 ppm in the ^{1}H NMR of macrocycle **1** to resonances of H_a and H_b, respectively. (We always observe OH groups hydrogen-bonded to ketimine N atoms to be downfield of those hydrogen-bonded to aldimine N atoms.) The peak at 8.36 ppm is the imine resonance (H_c); this is where we always observe imine resonances.

From the integration of the peak at 6.54 ppm, it may come from H_d or H_k. The other peak with the same integration appears at 6.88 ppm (it is overlapped by another peak.) H_d is positioned between two hydroxyl groups, so we expected this one to be the most upfield of the two. We verified that the peak at 6.45 ppm is indeed H_d by performing a deuterium exchange experiment. Upon exposure to MeOH-d_4 at elevated temperature, the proton at 6.54 ppm decreases in intensity relative to the other protons; the exchange of protons on benzene rings in resorcinol-based species has been observed previously. We also made the deuterated precursor to ensure that this assignment was correct.

There are three singlets between 6 and 7 ppm whose integrations are around 1.0. The chemical shifts of these three peaks are 6.84, 6.62 and 6.14 ppm, which must correspond to H_e, H_f and H_l. Because only H_e was shielded by phenyl ring, we attribute the signal at 6.14 ppm to H_e. As for the assignment of peaks **f** and **l**, we resorted to the 2D-ROESY spectrum shown in Figure S8**.** In Figure S8, there is a spin coupling between the signals at 6.62 and 3.92 ppm which corresponds to the –OC**H**$_2$- of the pentoxyl chain. However, there is no coupling found between peak at 6.84 ppm and signal of –OC**H**$_2$-. Therefore, the proton corresponding to signal at 6.62 ppm is

near to the $-OCH_2-$ group, which was attributed to H_f in macrocycle **1**. The signal at 6.84 ppm in the macrocycle was thus assigned to H_l.

There are two kinds of $-OCH_2-$ protons, whose signals appear as triplets at 3.92 and 3.59 ppm. From the 2D-ROESY in Figure S8, the more downfield signal coupled with resonance of H_f. We therefore attribute the signal at 3.92 ppm to H_m. The peak at 3.59 ppm coupled with resonance of H_e, and we assigned it as signal of H_n.

There are three kinds of protons on the mono-substituted phenyl ring that is attached to the ketimine, i.e. H_o, H_p and H_q. The resonance of H_o, H_p and H_q should be doublet, triplet and triplet, respectively. In addition, the integration of signal of H_q should be half of the other two proton. From the above information, we attributed peak **o**, **p** and **q** to H_o, H_p and H_q, respectively.

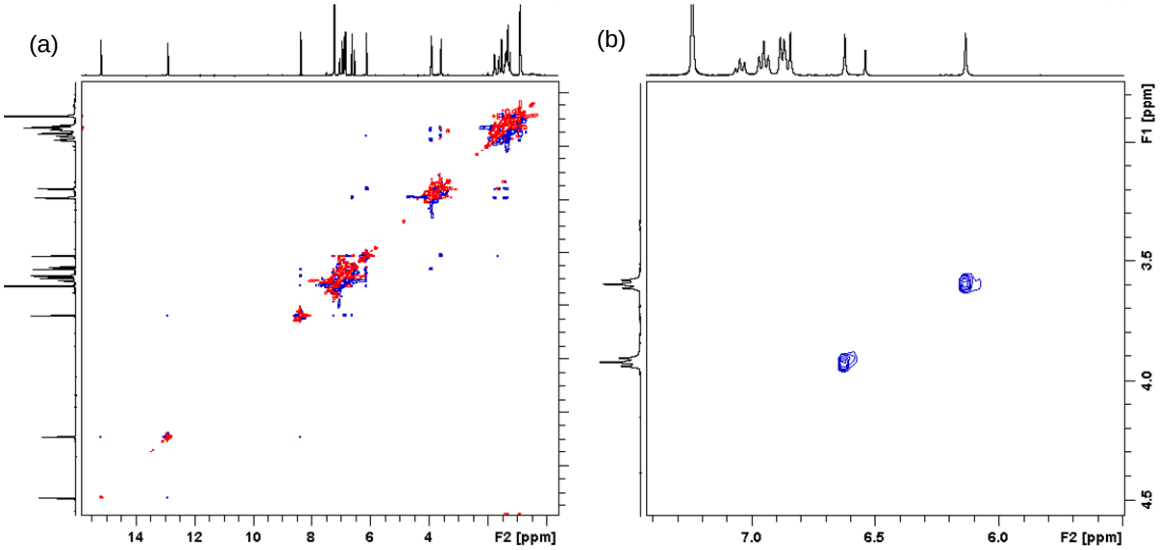

Figure S8. (a) 2D-ROESY spectrum of macrocycle **1** with a mixing time of 120 ms (400 MHz, $CDCl_3$, 298K). (b) Enlarged spectrum from 2.8 ppm to 4.5 ppm (F1) and from 5.5 ppm to 7.4 ppm (F2).

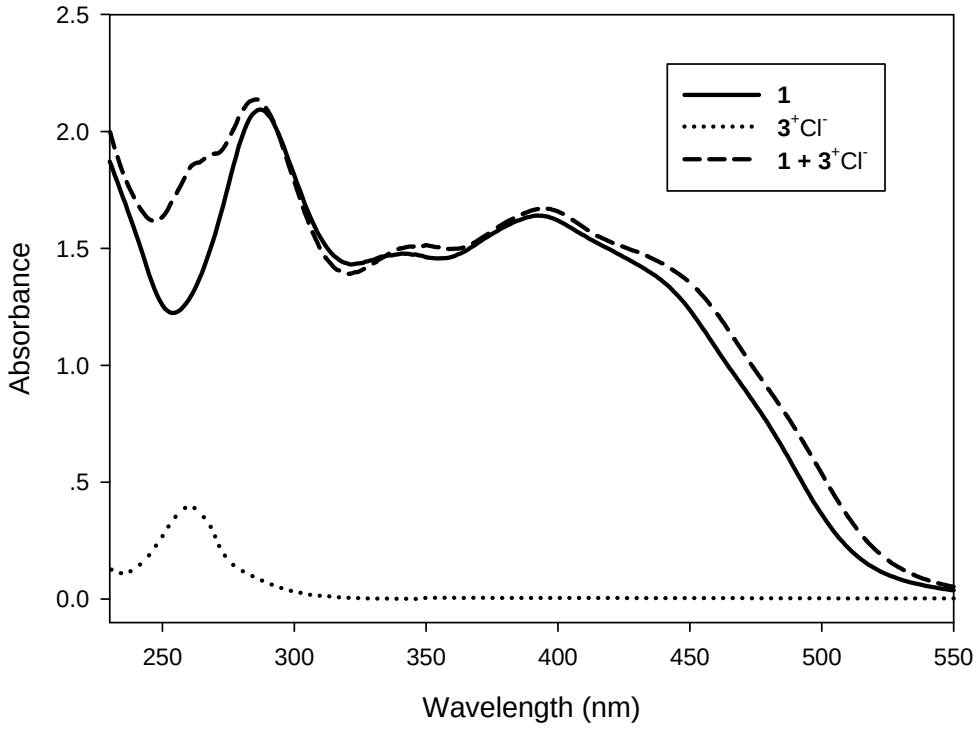

Figure S9. UV-vis spectrum (1.0 cm cell, 298K, CH_2Cl_2) of 0.025 mM macrocycle **1** (solid line), 0.141 mM **3**$^+$Cl$^-$ (dotted line) and mixture of 0.025 mM macrocycle **1** and 0.141 mM **3**$^+$Cl$^-$ (dashed line).

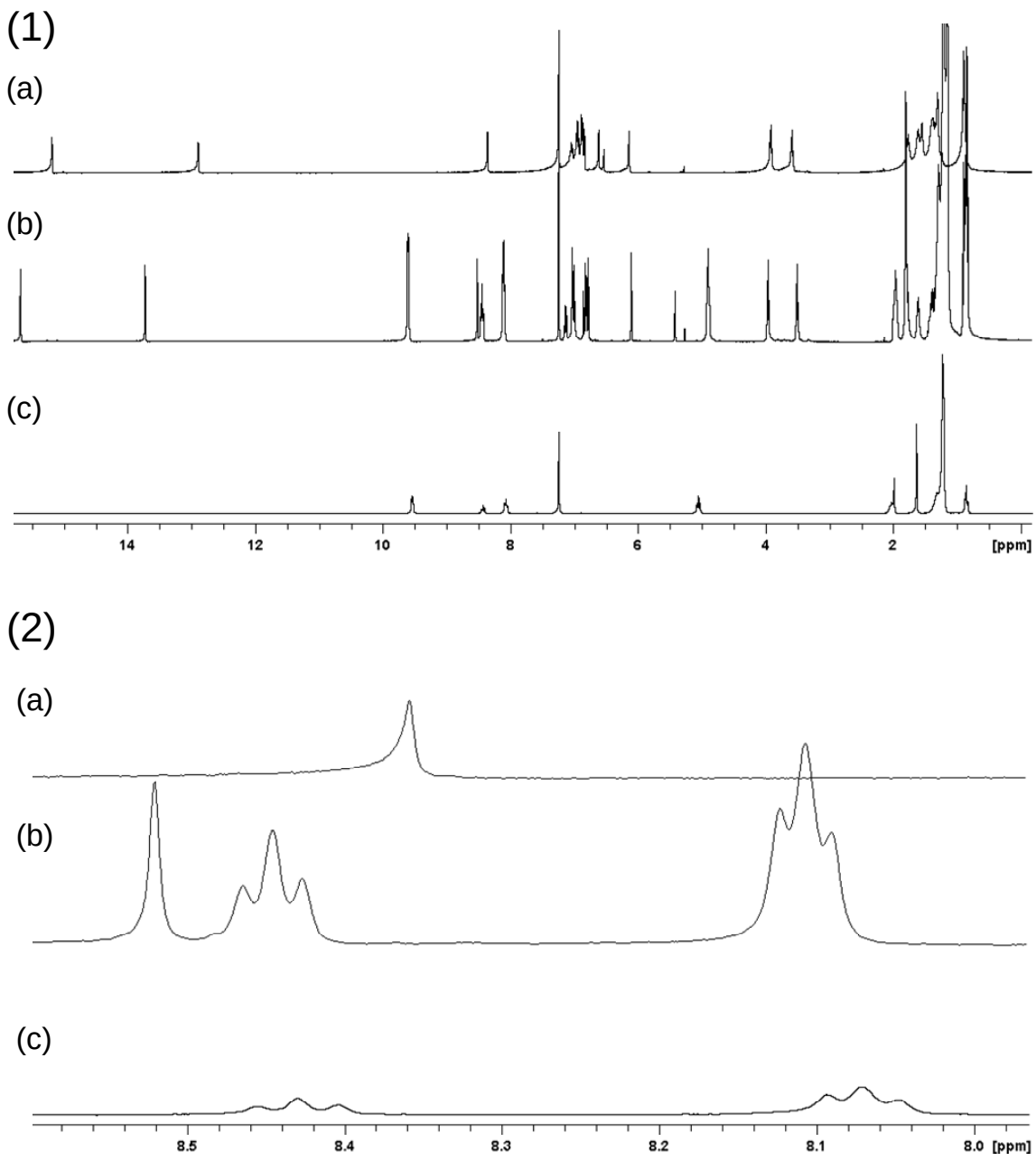

Figure S10. Top: ^{1}H NMR spectra of (a) macrocycle **1**; (b) mixture of macrocycle **1** and cetylpyridinium chloride ([**3**$^{+}$·Cl^{-}]:[**1**] = 5:1); and (c) cetylpyridinium chloride (**3**$^{+}$·Cl^{-}). Bottom: Same spectra shown from 8.0 to 8.6 ppm. (400 MHz, $CDCl_3$, 298 K)

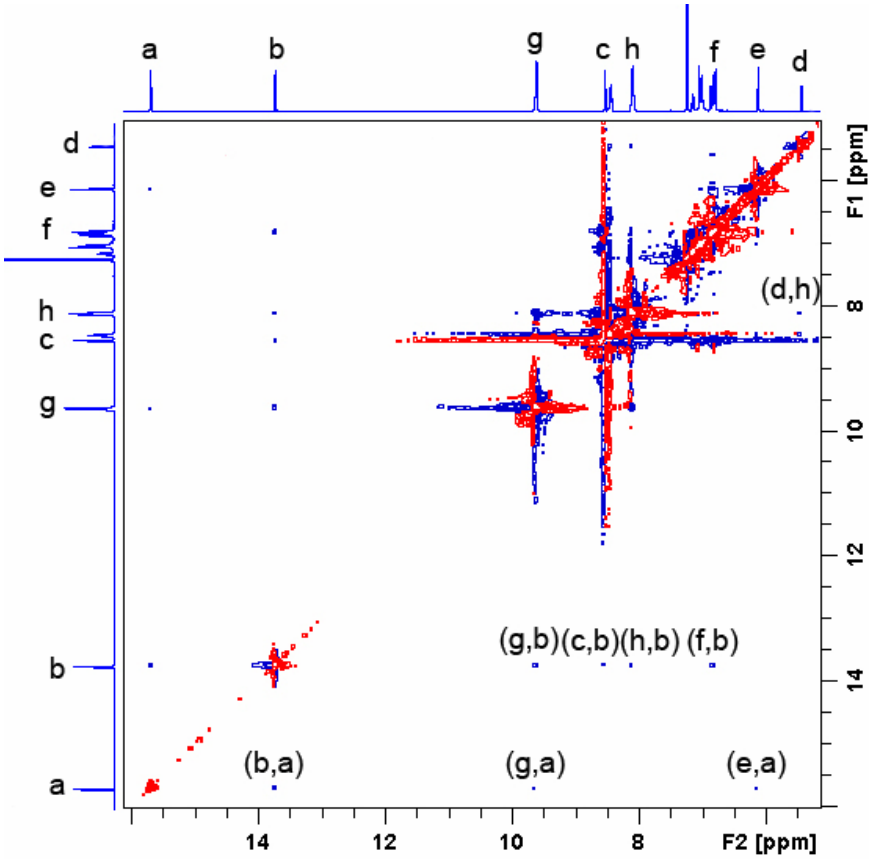

Figure S11. 2D-ROESY spectrum of the host-guest complex formed by macrocycle **1** and cetylpyridinium chloride $\mathbf{3}^{+}\cdot Cl^{-}$ with a mixing time of 120 ms (400 MHz, $CDCl_3$, 298 K).

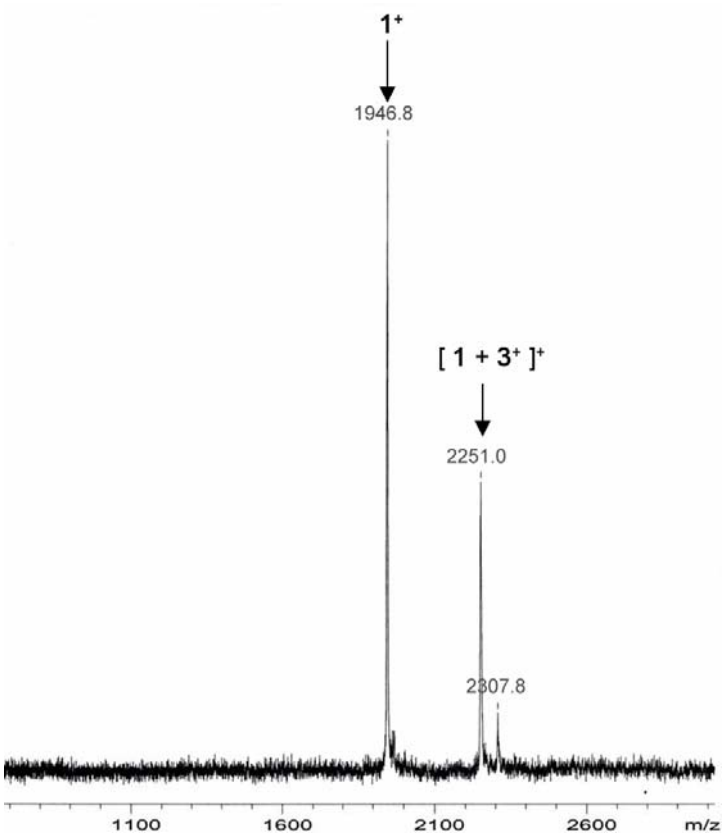

Figure S12. MALDI-TOF mass spectrum of host-guest complex $\mathbf{3}^{+} \subset \mathbf{1}$.

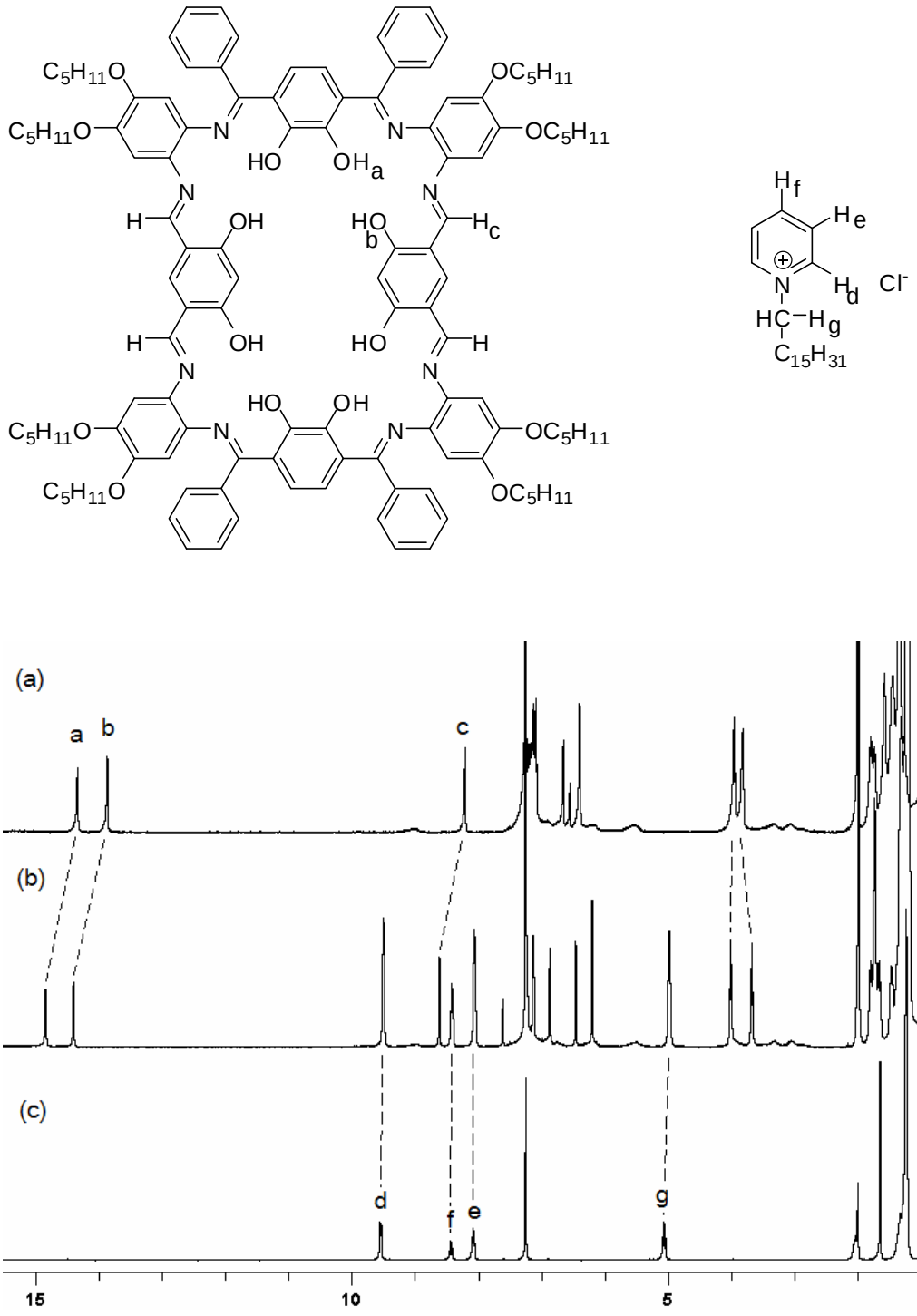

Figure S13. ^{1}H NMR spectra of (a) macrocycle **2**, (c) cetylpyridinium chloride and (b) the mixture with [**3**$^{+}$·Cl^{-}]:[**2**] = 6:1 (400 MHz, $CDCl_3$, 298 K).

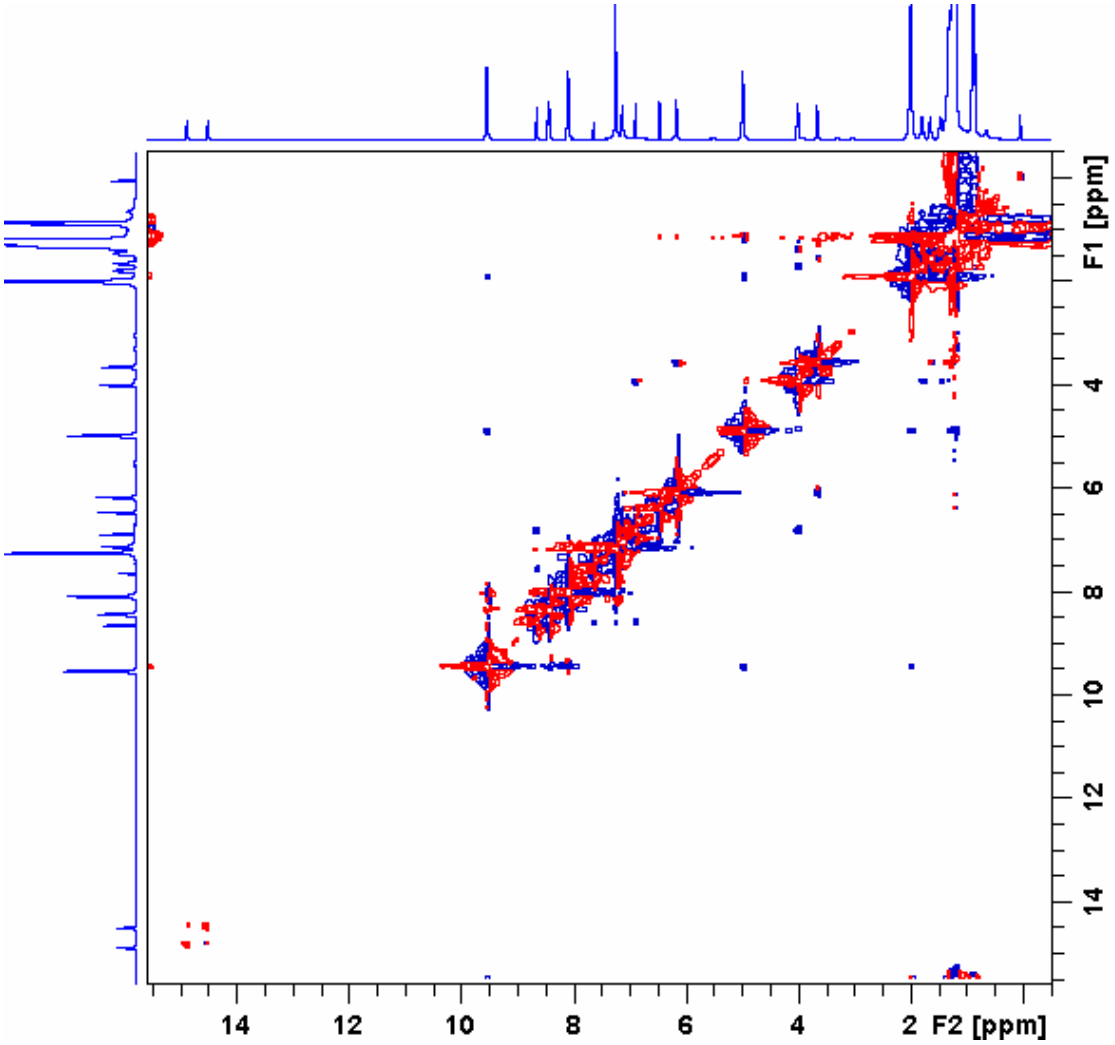

Figure S14. 2D-ROESY spectrum of complex formed by macrocycle **2** and cetylpyridinium chloride $\mathbf{3}^{+}\cdot Cl^{-}$ with a mixing time of 120 ms (400 MHz, $CDCl_3$, 298K).

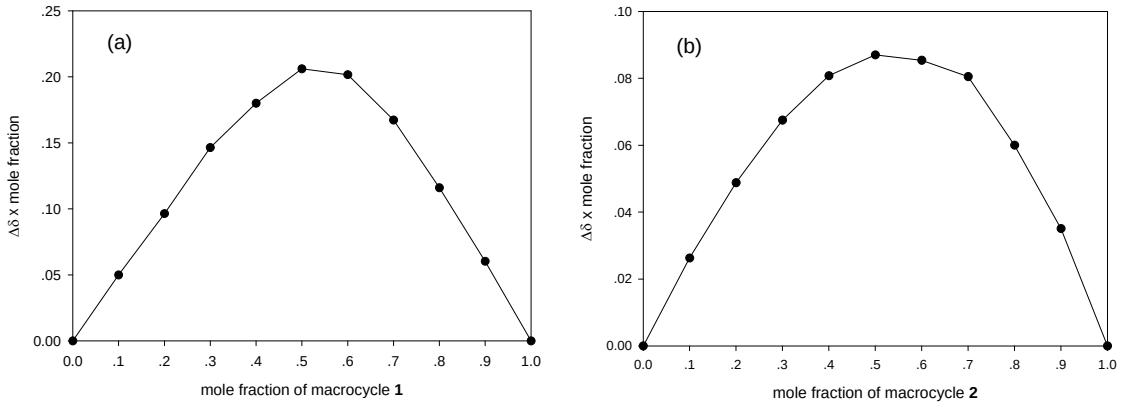

Figure S15. Job plots of (a) $\mathbf{3}^{+}\subset\mathbf{1}$ and (b) $\mathbf{3}^{+}\subset\mathbf{2}$ (400 MHz, $CDCl_3$, 298 K).

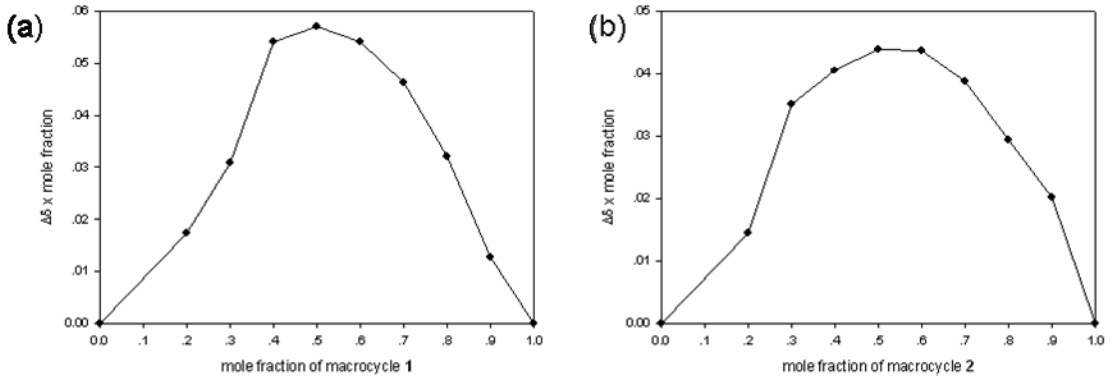

Figure S16. (a) Job plot of macrocycle **1** with methyl viologen in $CDCl_3/CD_3OD$ (3:1). (b) Job plot of macrocycle **2** with methyl viologen in $CDCl_3/CD_3OD$ (3:1).

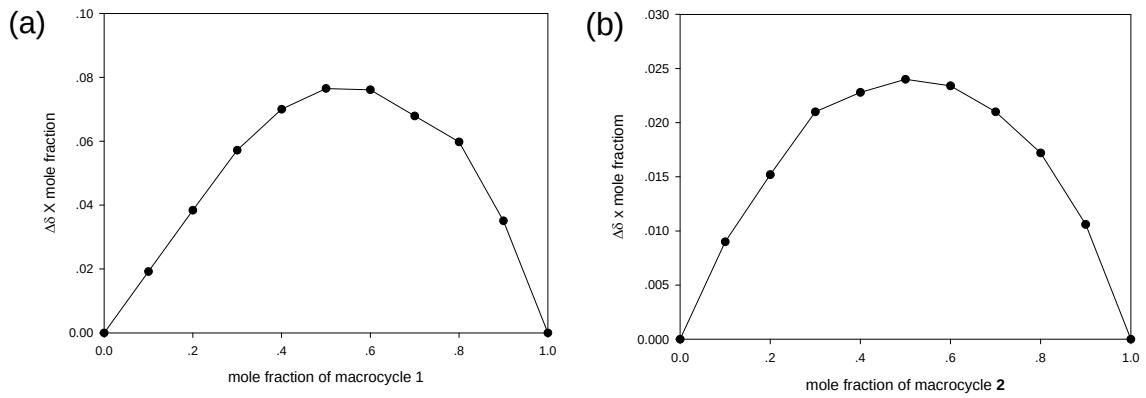

Figure S17. (a) Job plot of macrocycle **1** with cetyltrimethylammonium bromide ($\mathbf{4}^{+}\cdot Br^{-}$)in $CDCl_3$. (b) Job plot of macrocycle **2** with $\mathbf{4}^{+}\cdot Br^{-}$ in $CDCl_3$.

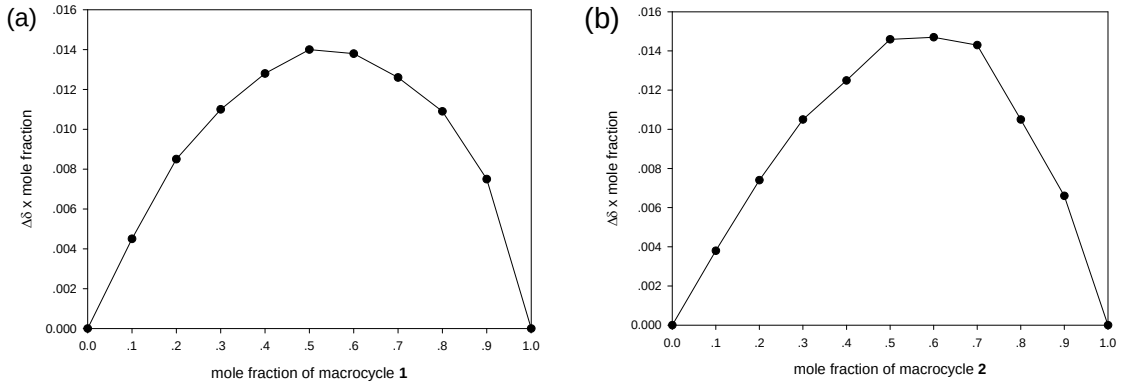

Figure S18. (a) Job plot of macrocycle **1** with tetrabutylammonium bromide ($\mathbf{5}^{+}\cdot Br^{-}$) in $CDCl_3$. (b) Job plot of macrocycle **2** with $\mathbf{5}^{+}\cdot Br^{-}$ in $CDCl_3$.

(a)

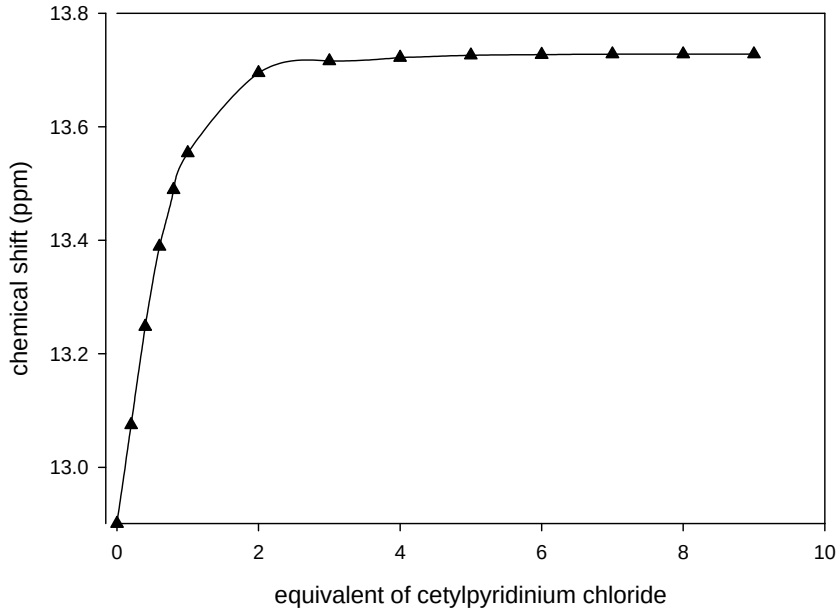

(b)

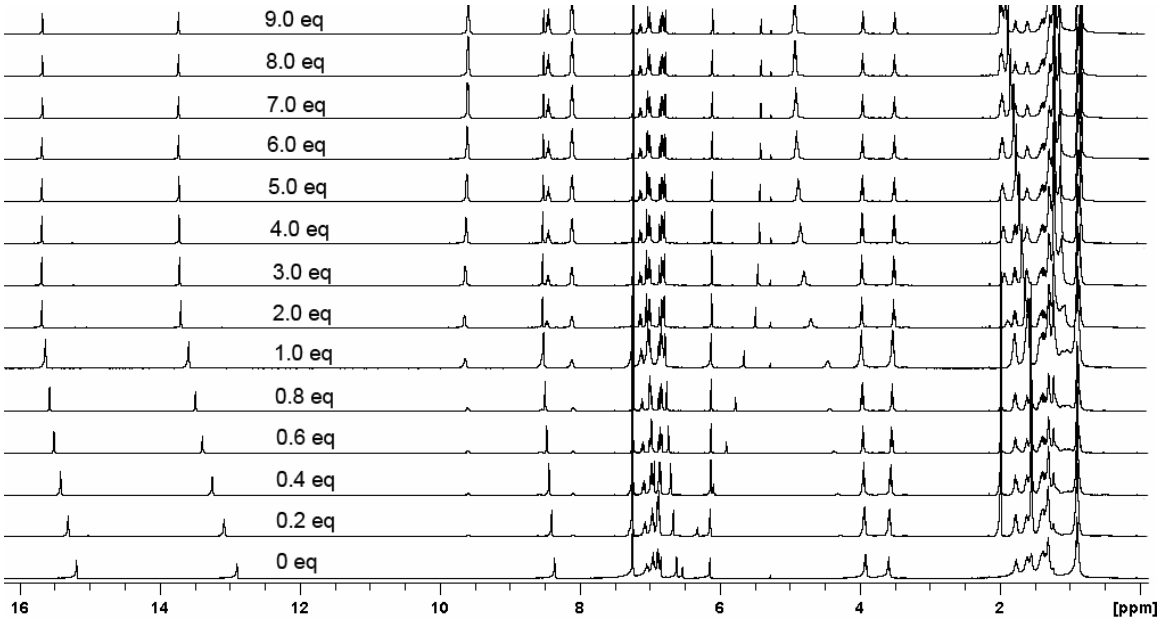

Figure S19. Titration curve (a) and stacked ^{1}H NMR spectra (b) of macrocycle **1** with cetylpyridinium chloride $\mathbf{3}^{+}\cdot Cl^{-}$ (400 MHz, $CDCl_3$, 298 K).

(a)

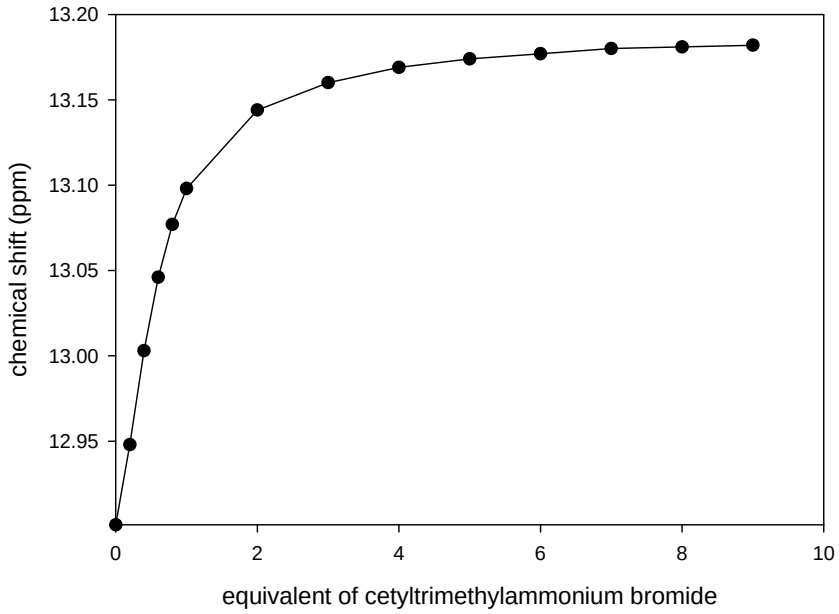

(b)

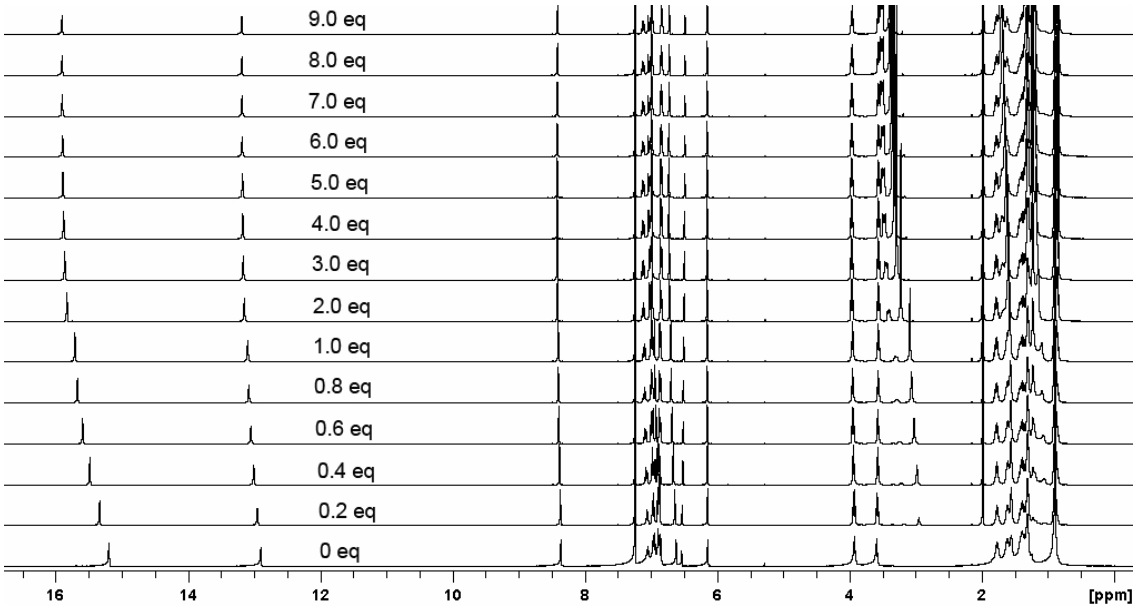

Figure S20. Titration curve (a) and stacked ^{1}H NMR spectra (b) of macrocycle **1** with cetyltrimethylammonium bromide $\mathbf{4}^{+}\cdot Br^{-}$ (400 MHz, $CDCl_3$, 298 K).

(a)

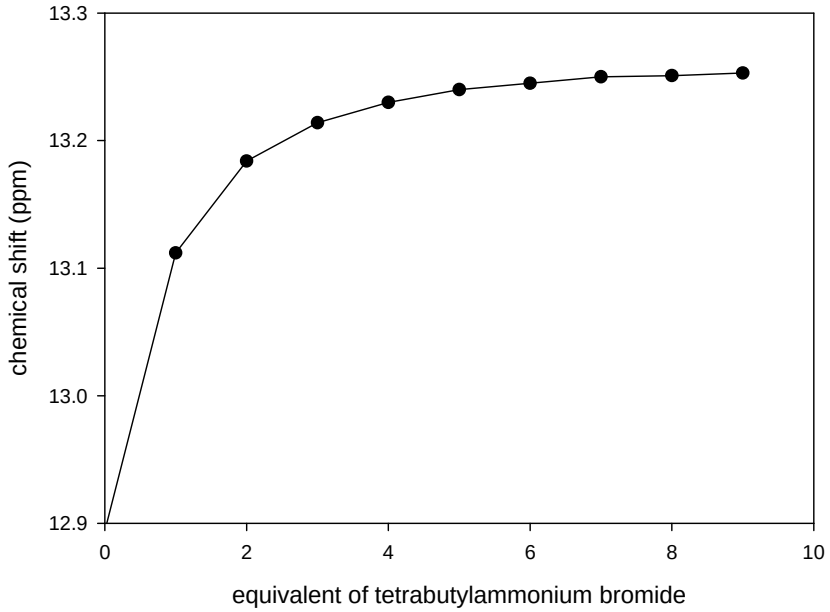

(b)

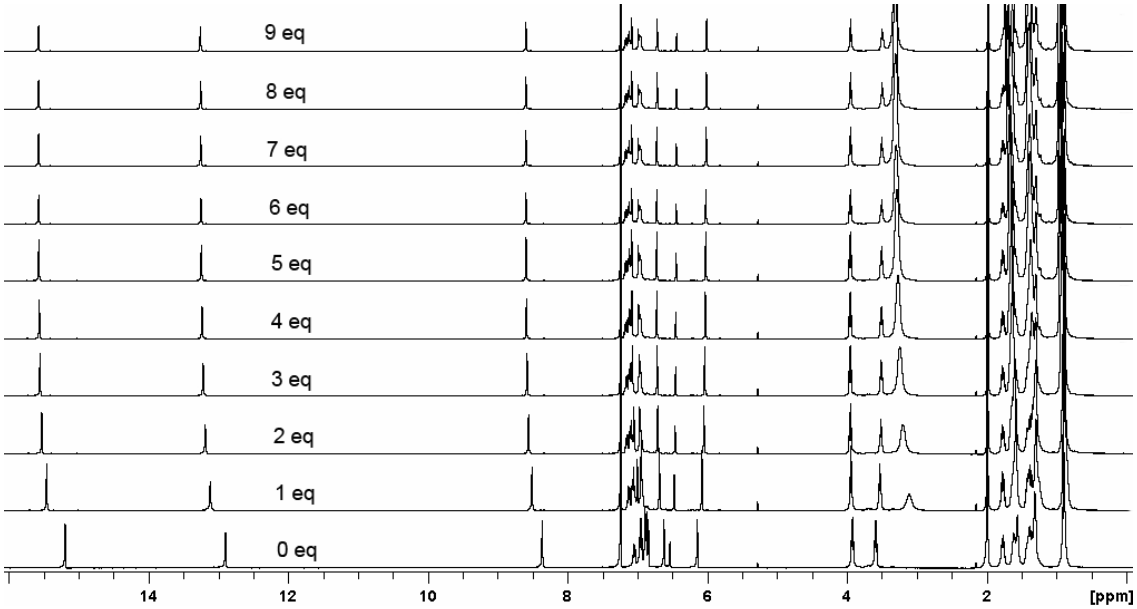

Figure S21. Titration curve (a) and stacked ^{1}H NMR spectra (b) of macrocycle **1** with tetrabutylammonium bromide $\mathbf{5}^{+}\cdot Br^{-}$ (400 MHz, $CDCl_3$, 298 K).

(a)

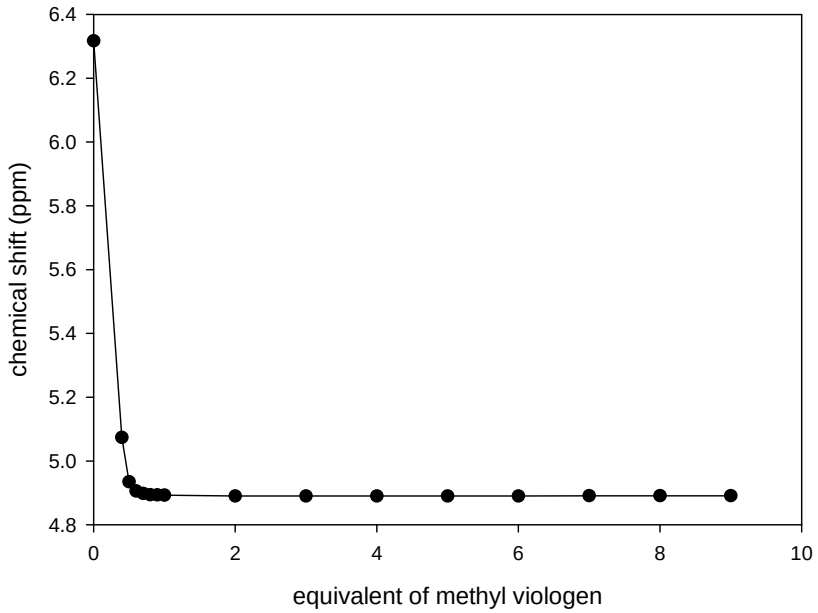

(b)

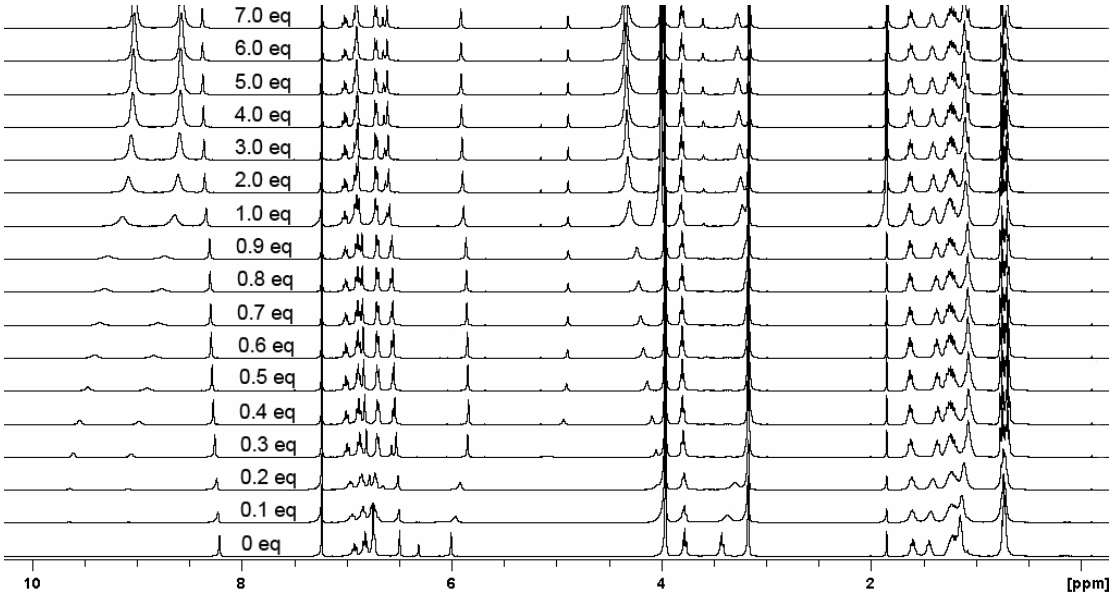

Figure S22. Titration curve (a) and stacked ^{1}H NMR spectra (b) of macrocycle **1** with methyl viologen dichloride $\mathbf{6}^{2+}\cdot 2Cl^{-}$ in $CDCl_3/CD_3OD$ (3 : 1) (400 MHz, 298 K).

(a)

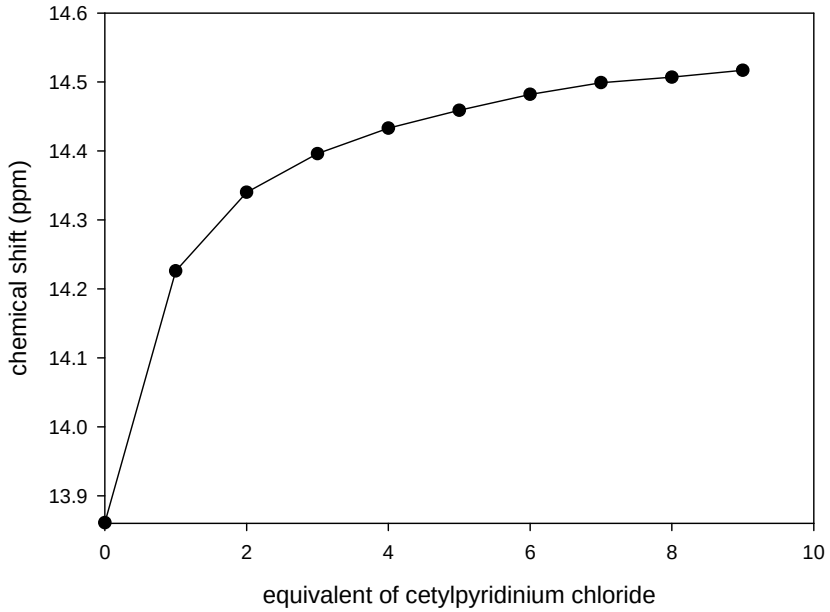

(b)

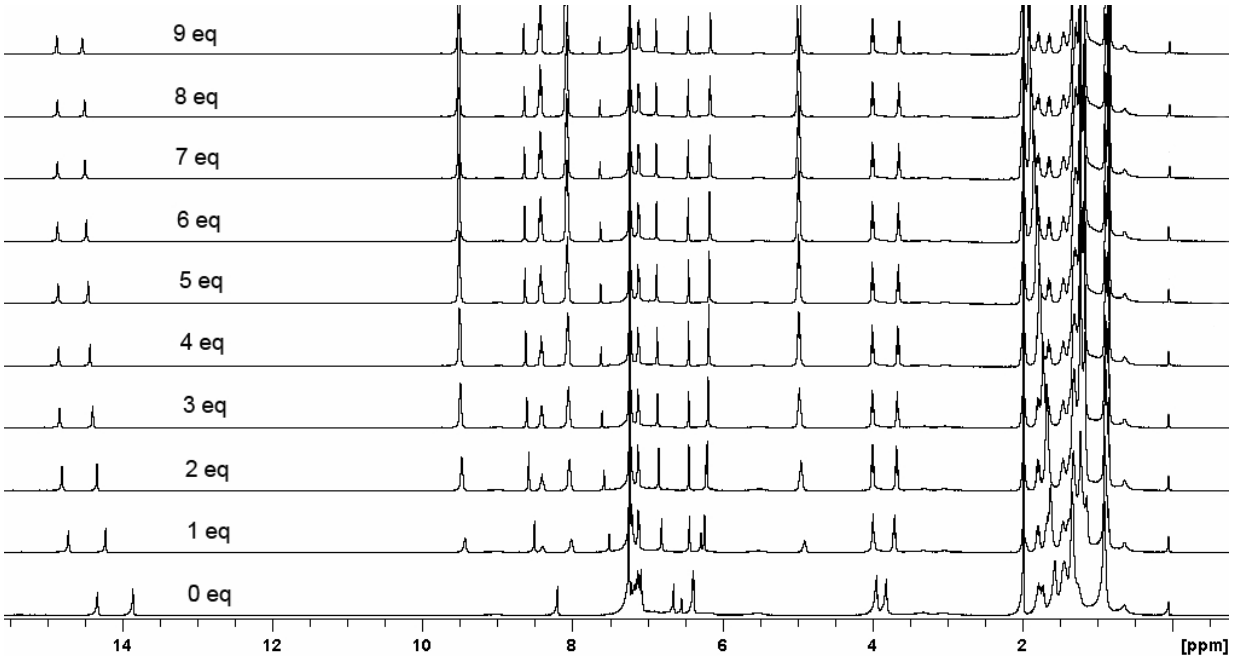

Figure S23. Titration curve (a) and stacked ^{1}H NMR spectra (b) of macrocycle **2** with cetylpyridinium chloride $\mathbf{3}^{+}\cdot Cl^{-}$ (400 MHz, $CDCl_3$, 298 K).

(a)

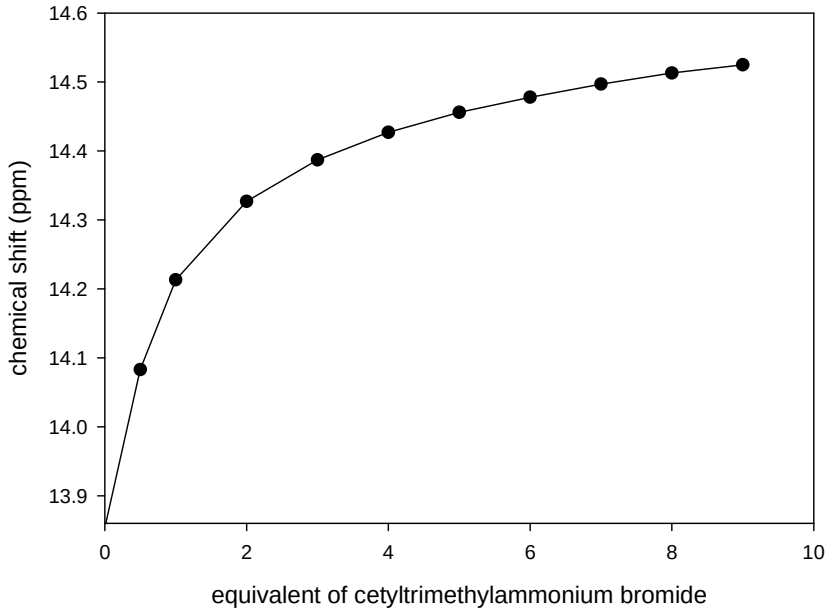

(b)

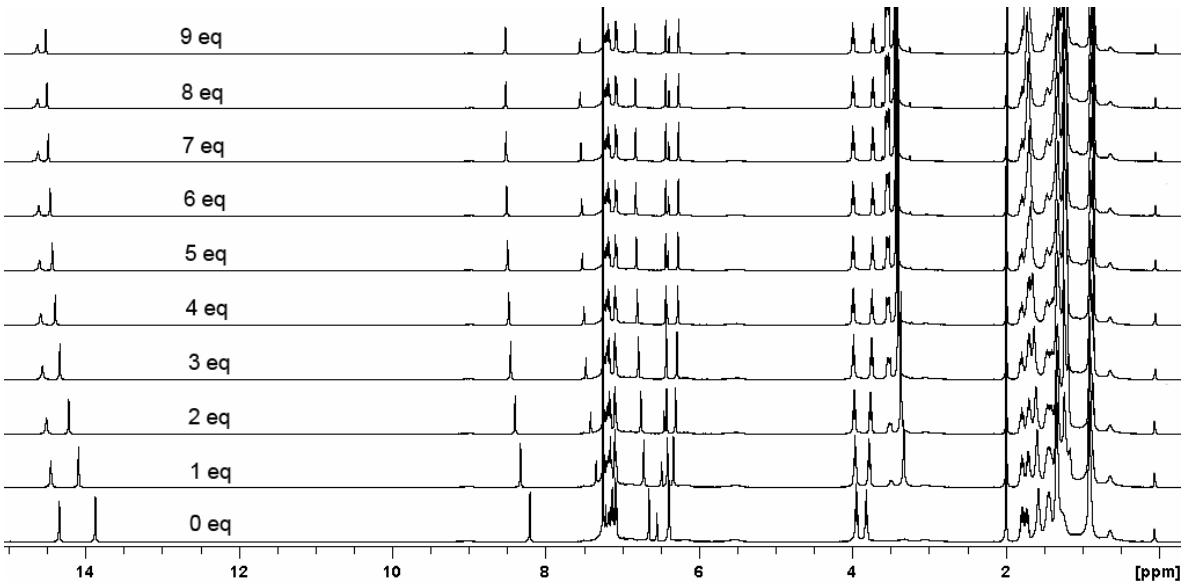

Figure S24. Titration curve (a) and stacked ^{1}H NMR spectra (b) of macrocycle **2** with cetyltrimethylammonium bromide $\mathbf{4}^{+}\cdot Br^{-}$ (400 MHz, $CDCl_3$, 298 K).

(a)

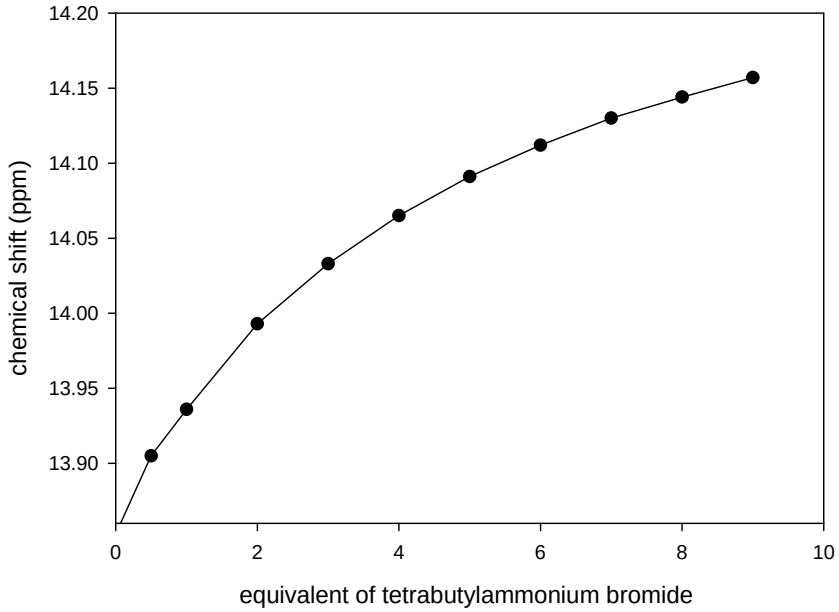

(b)

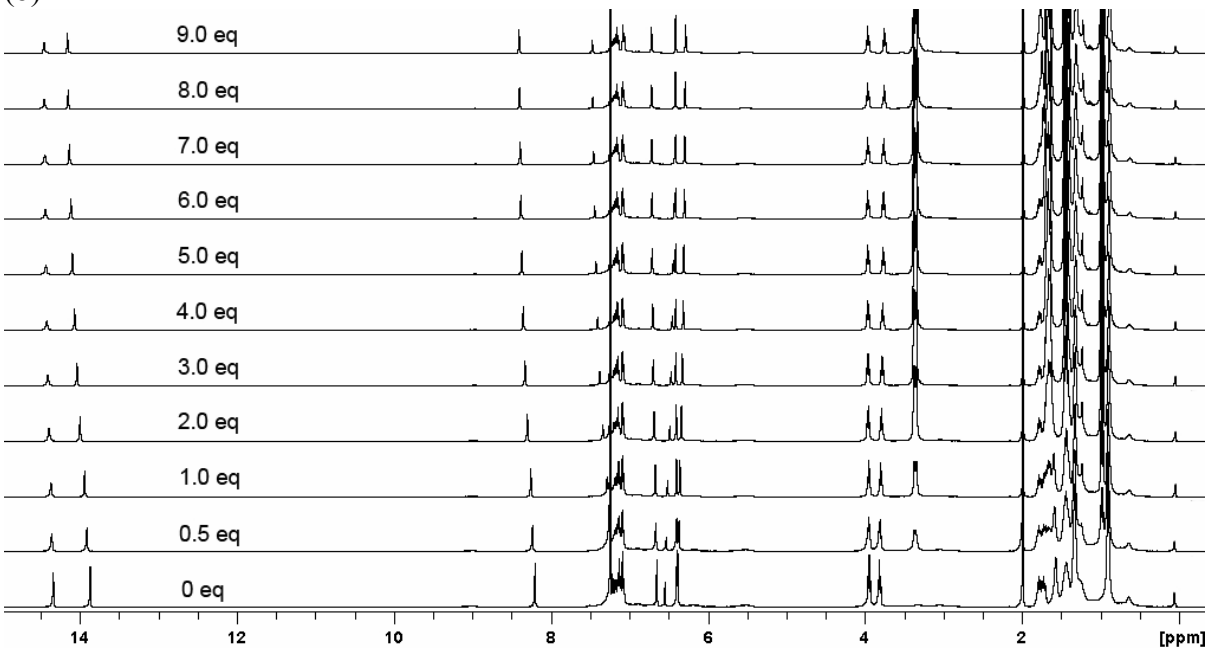

Figure S25. Titration curve (a) and stacked ^{1}H NMR spectra (b) of macrocycle **2** with tetrabutylammonium bromide $\mathbf{5}^{+}\cdot Br^{-}$ (400 MHz, $CDCl_3$, 298 K).

(a)

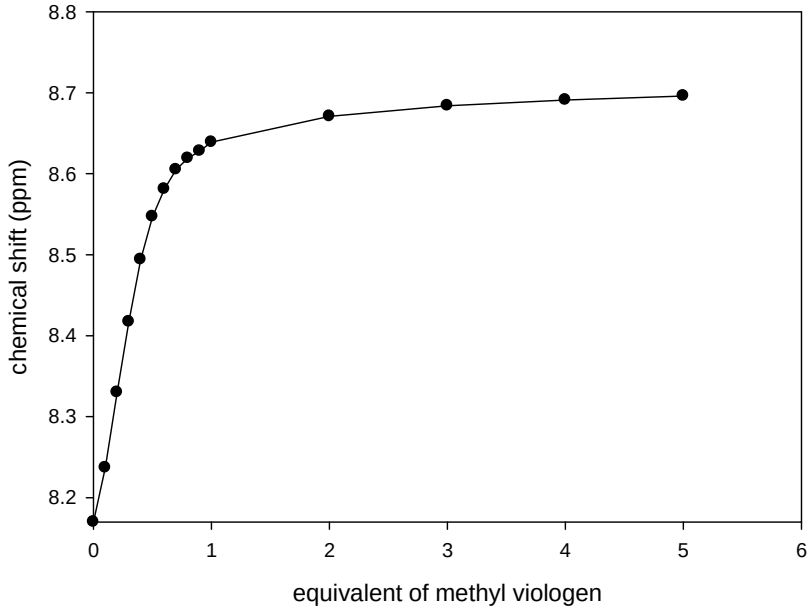

(b)

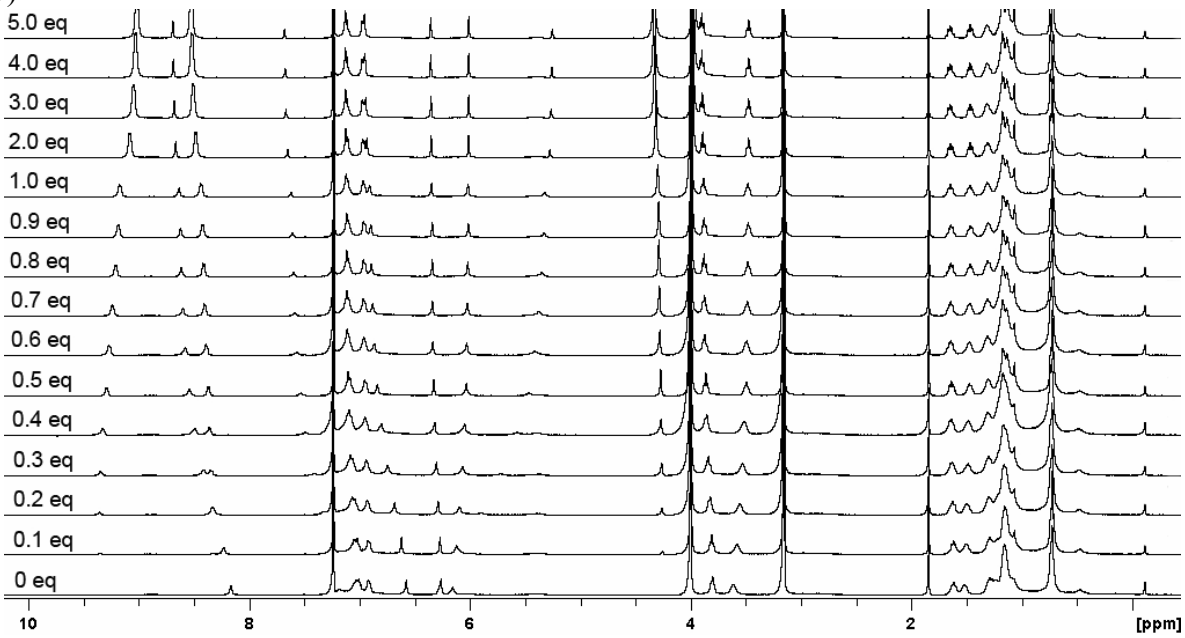

Figure S26. Titration curve (a) and stacked ^{1}H NMR spectra (b) of macrocycle **2** with methyl viologen dichloride $\mathbf{6}^{2+}\cdot 2Cl^{-}$ in $CDCl_3/CD_3OD$ (3:1) (400 MHz, 298 K).

(a)

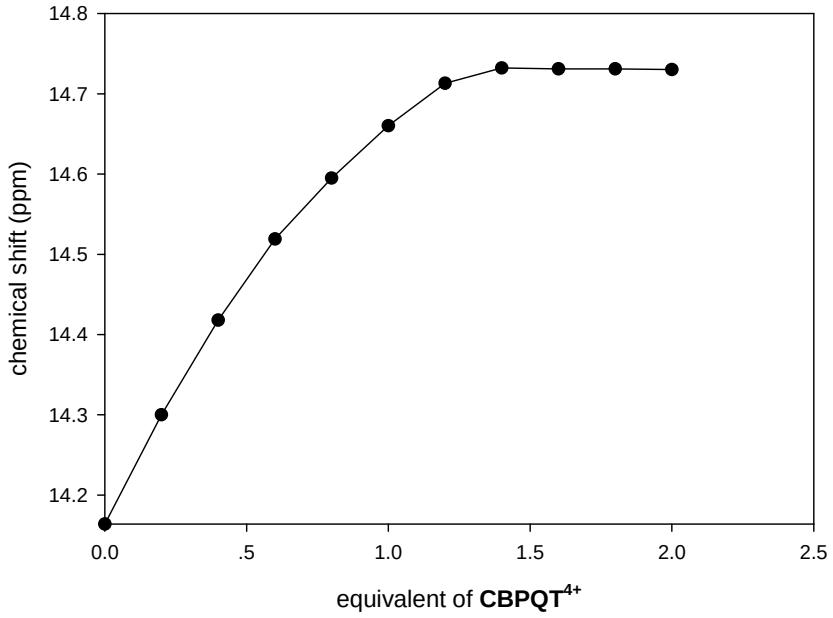

(b)

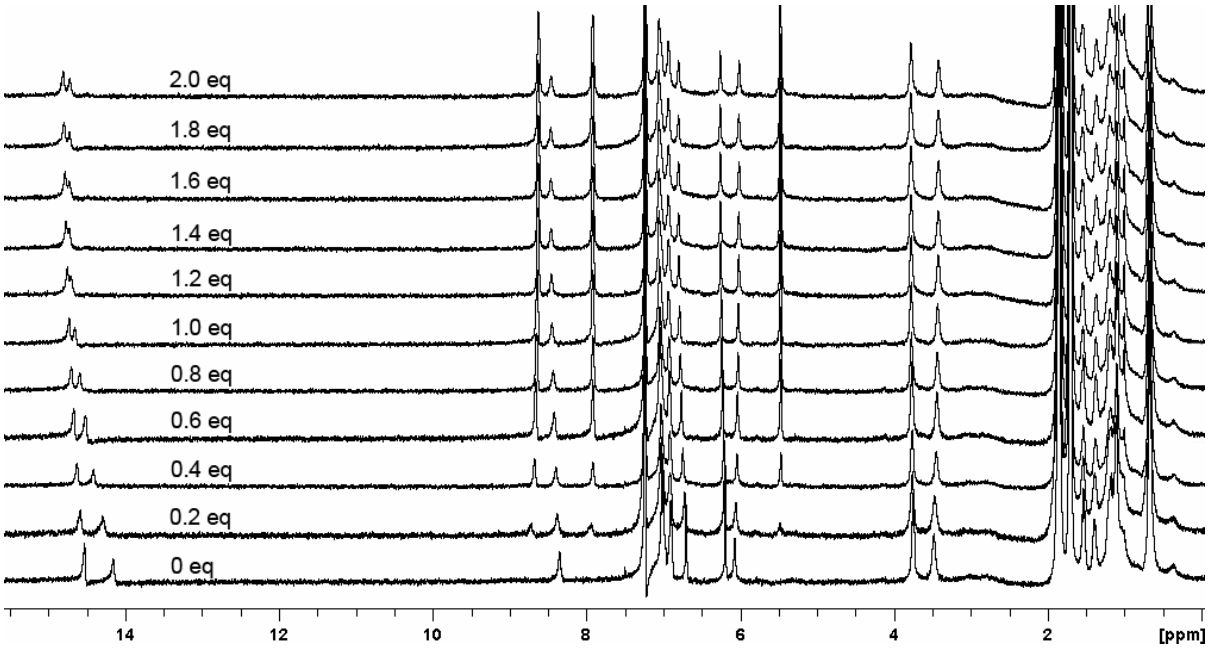

Figure S27. Titration curve (a) and stacked ^{1}H NMR spectra (b) of macrocycle **7** with **CBPQT**$^{4+}$ $(PF_6)_4$ in $CDCl_3/CD_3CN$ (1:1) (400 MHz, 298 K).

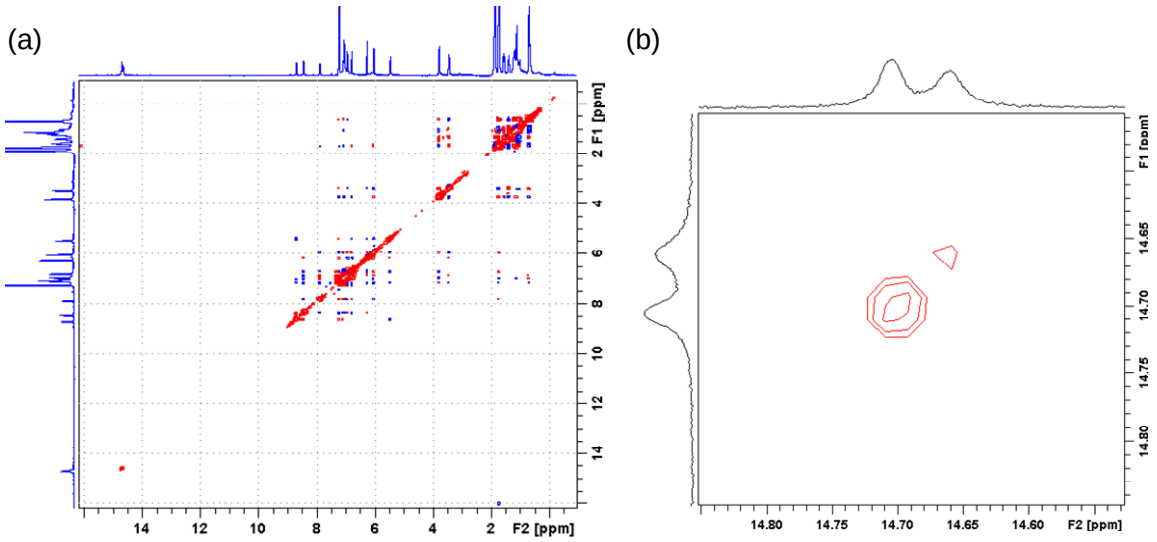

Figure S28. (a) 2D-ROESY NMR spectrum of complex formed by macrocycle **7** and **CBPQT**$^{4+}$ $(PF_6)_4$ in $CDCl_3/CD_3CN$ (1:1) with a mixing time of 120 ms (400 MHz, 298 K). (b) Enlarged spectrum from (a) from 14.55 to14.85 ppm.

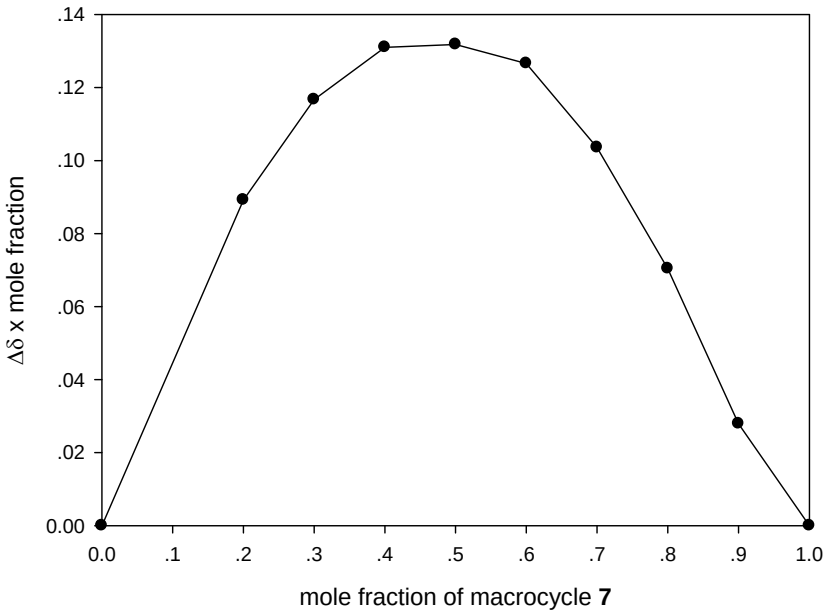

Figure S29. Job plot of macrocycle **7** with **CBPQT**$^{4+}$ $(PF_6)_4$ in 1:1 $CDCl_3/CD_3CN$ (400 MHz, 298 K)

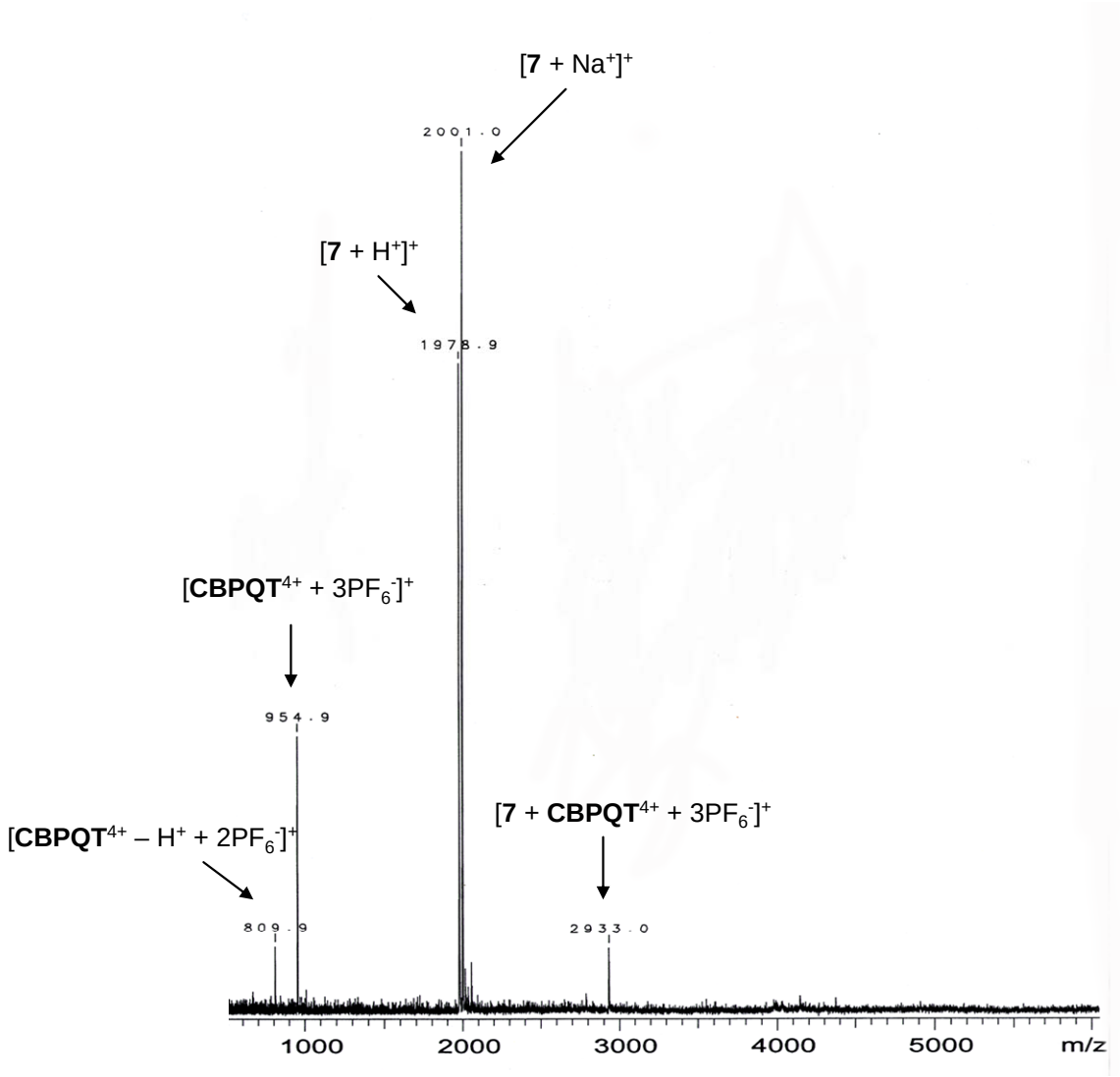

Figure S30. MALDI-TOF mass spectrum of complex formed by **CBPQT**$^{4+}$ $(PF_6)_4$ and **7**

Characterization Data for Macrocycle 7

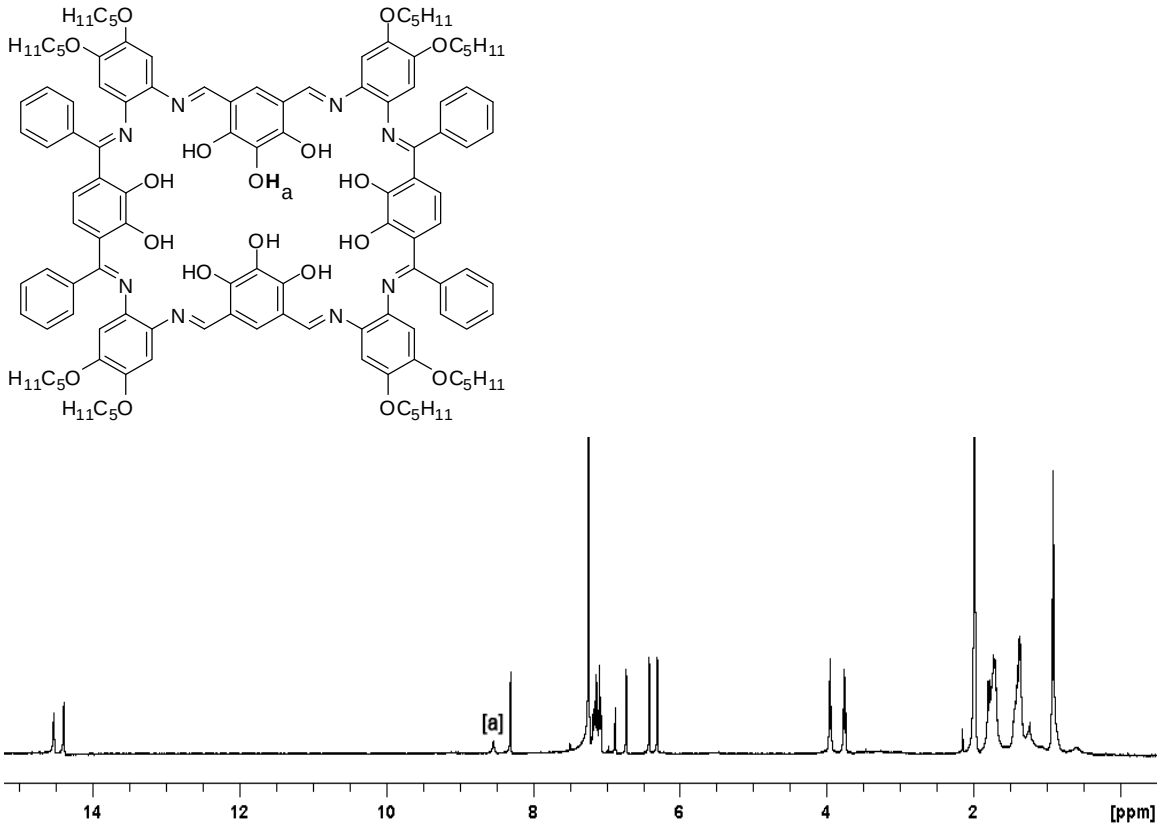

Figure S31. ^{1}H NMR spectrum of macrocycle **7** (400 MHz, $CDCl_3$, 298 K) (The peak [a] at 8.562 ppm is the signal of H_a. This peak is only observed in some capacity when the deuterated solvent is very dry.)

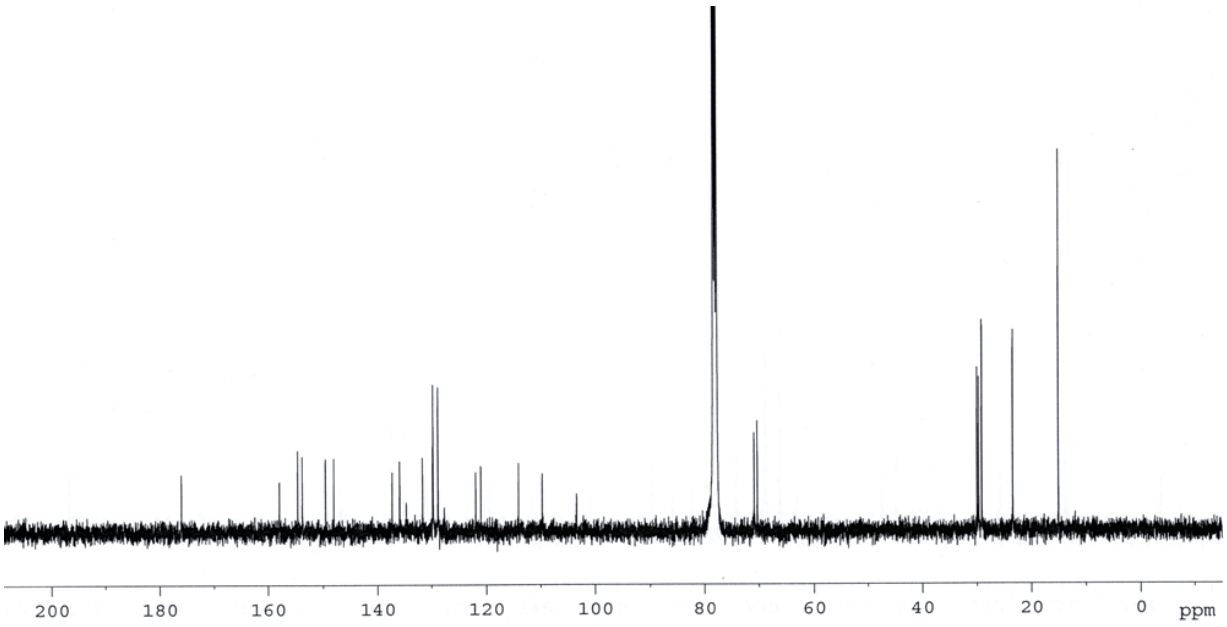

Figure S32. ^{13}C NMR spectrum of macrocycle **7** (100.6 MHz, $CDCl_3$, 298 K)

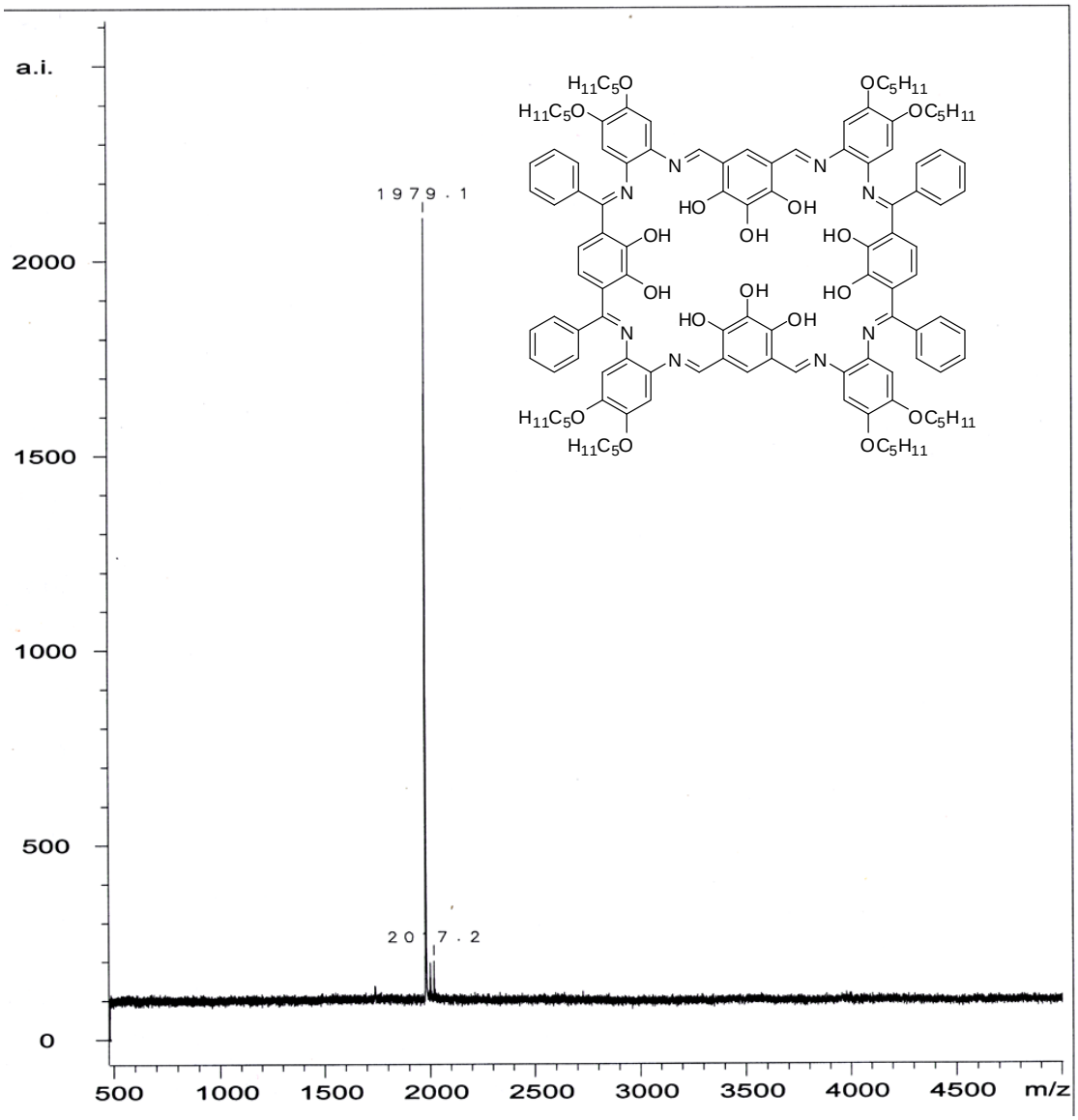

Figure S33. MALDI-TOF mass spectrum of macrocycle **7**

References

[1] B. Odell, M. V. Reddington, A. M. Z. Slawin, N. Spencer, J. F. Stoddart and D. J. Williams, *Angew. Chem., Int. Ed. Engl*., 1988, **27**, 1547.
[2] P. D. Frischmann, J. Jiang, J. K.-H. Hui, J. J. Grzybowski, M. J. MacLachlan, *Org. Lett*., 2008, **10**, 1255.
[3] G. Henning, H. Juergen, W. Hauptlab and B. A.-G. Leverkusen, *Justus Liebigs Ann. Chem.*, 1978, **2**, 345.
[4] P. Job, *Ann. Chim.*, 1928, **9**, 113.
[5] R. S. Macomber, *J. Chem. Ed.*, 1992, **69**, 375.
[6] M. Gerhards, C. Unterberg and S. Schumm, *J. Chem. Phys.*, 1999, **111**, 7966.
[7] A. J. Gallant and M. J. MacLachlan, *Angew. Chem. Int. Ed.*, 2003, **42**, 5307.